Canadian Journal of Earth Sciences

Research Article

Edmontosaurus from the Rocky Mountain foothills, Alberta, and its chronostratigraphic position in the Late Cretaceous Brazeau Formation and correlative units in western Canada

Aaron J. van der Reest[a], **S. Andrew DuFrane**[b], **Alberto V. Reyes**[b], **Philip J. Currie**[c], **and Jennifer J. Scott**[a,d]

[a]Department of Geological Sciences, University of Saskatchewan, Saskatoon, SK S7N 5E2, Canada; [b]Department of Earth & Atmospheric Sciences, University of Alberta, Edmonton, AB T6G 2E3, Canada; [c]Department of Biological Sciences, University of Alberta, Edmonton, AB T6G 2E9, Canada; [d]Department of Earth & Environmental Sciences, Mount Royal University, Calgary, AB T3E 6K6, Canada

Corresponding author: **Aaron J. van der Reest** (email: kxb604@usask.ca)

Abstract

The Upper Cretaceous Brazeau Formation (early Campanian–early Maastrichtian) near Hinton, AB, preserves dinosaur fossils associated with fluvial and lacustrine palaeoenvironments during a transgressive–regressive cycle within the Western Interior Seaway. Here, the first description of vertebrate remains, hadrosaurid footprints, and radiometric age constraints from the Brazeau Formation are presented. Multiple dinosaur elements were recovered from a new bonebed, including a left postorbital and a partial right postorbital representing *Edmontosaurus* sp. based on an enlarged postorbital fossa. These are the first dinosaur elements diagnosable to the genus level to have been described from the Brazeau Formation; vertebrate remains have not previously been described from this formation. Eight tephras lie between ~24 and ~263 m above the Bennett Bonebed. Seven yielded statistically indistinguishable weighted-average laser ablation zircon $^{206}Pb/^{238}U$ dates between 70.14 ± 0.38 Ma (23.75 m) and 69.60 ± 0.35 Ma (~262.60 m). A Bayesian age-depth model based on the zircon U–Pb dates yields a bonebed age of 70.17 ± 0.42|0.38 Ma and a median sedimentation rate of ~450 m/Myr across the ~240 m of measured section. The age of the Bennett Bonebed is, therefore, equivalent to the upper Tolman Member of the Horseshoe Canyon Formation, placing it in the middle Maastrichtian, ~1.3 Ma after *Edmontosaurus regalis* is proposed to have been extirpated from Alberta, and within the >2 Ma hiatus of the genus from the fossil record of northwestern North America.

Key words: *Edmontosaurus*, Palaeontology, Brazeau Formation, Maastrichtian, radiometric dates, dinosaur distribution

Introduction

Edmontosaurus (Lambe 1917), a large saurolophine hadrosaur known from the northern half of Laramidia, is one of the most common hadrosaurs from the uppermost Campanian and Maastrichtian (Lambe 1920; Eberth et al. 2013; Bell and Campione 2014; Bell et al. 2014; Evans et al. 2015; Campbell et al. 2020). *Edmontosaurus regalis* is the geologically oldest known species (~72.5–71.5 million years ago (Ma)) and is currently the only species of *Edmontosaurus* known from Alberta (Eberth et al. 2013, 2014; Bell and Campione 2014). Since hadrosaurs can be especially useful for dinosaur biostratigraphy, such as *Corythosaurus*, *Lambeosaurus*, and *Prosaurolophus* in the Dinosaur Park Formation (Mallon et al. 2012), and *Edmontosaurus*, *Hypacrosaurus*, and *Saurolophus* in the Horseshoe Canyon Formation (HCF) (Eberth et al. 2013), establishing their stratigraphic range and distribution across a spectrum of depositional environments is particularly important. A thorough consideration of sedimentological evidence for palaeoenvironments of fossil sites and how they change through time should be an integral component of biostratigraphic and palaeoecological studies. The vertebrate palaeontological record, set within this context, can be applied to understanding ecological forces on dinosaurs that affected their evolution (e.g., climate change and sea-level change), and it can provide insights into the distribution of suitable habitats across the Late Cretaceous landscape, potentially improving our understanding of migration within taxa. With this approach, this study reports new examples of *Edmontosaurus* from the latest Cretaceous Brazeau Formation of Alberta, and aims to establish its chronostratigraphic position, interpret the associated palaeoenvironments, and consider the potential basin-scale controls on the timing and distribution of this genus in western Canada.

Other known species of *Edmontosaurus* include a probable separate species from the Prince Creek Formation (originally referred to as *Ugrunaaluk kuukpikensis* ~69.2 Ma), which is cur-

rently only known from northern Alaska (Mori et al. 2016; Takasaki et al. 2020), and the youngest species, *Edmontosaurus annectens* (~67.5–66 Ma), known from southern Saskatchewan and the northern mid-west United States (Campione and Evans 2011). Therefore, the temporal distributions of each species leave time gaps of a couple of million years (2.3 and 1.7 million years (Myr), respectively) between these species. During these temporal gaps, the geographic distribution of the genus *Edmontosaurus* has remained unknown. Previously known examples of *Edmontosaurus* are preserved in deposits representing relatively wet coastal plain areas adjacent to the Western Interior Seaway and palaeo-Arctic Ocean (Eberth et al. 2013; Fanti et al. 2013; Bell et al. 2014; Evans et al. 2015; Mori et al. 2016; Campbell et al. 2020).

The known distribution of *Edmontosaurus regalis* in Alberta extends from the Peace River Region in the northwest (lower Unit 4 of the Wapiti Formation (WF); Bell et al. 2014; Fanti et al. 2022), south through Edmonton and Drumheller (Horsethief Member of the HCF; Eberth et al. 2013), and into southern Alberta near Lethbridge (lower St. Mary River Formation; Campbell et al. 2020). No specimens of hadrosaurs or other dinosaurs have previously been described from the time-equivalent Brazeau Formation (~80–67 Ma) in the Rocky Mountains and foothills region, in part due to limited exposure in river cuts and remote field areas. Each of the units in which *Edmontosaurus regalis* is known represents coastal plain or deltaic deposits that preserve coal seams in close stratigraphic proximity to recovered specimens (Russell and Chamney 1967; Eberth et al. 2013; Bell et al. 2014; Campbell et al. 2020). The top of the "middle" Brazeau Formation, in which the *Edmontosaurus* specimens reported here were recovered, lacks coal, and instead preserves a thick (>40 m) stratigraphic succession of lake-margin environments. The depositional setting is similar to those reported from other regions from which *Edmontosaurus* has been recovered in that it represents a well vegetated and wet palaeoenvironment; however, no coal is associated.

The Brazeau Formation (Saunders Group) correlates to the Belly River Group (Foremost, Oldman, Dinosaur Park formations), Bearpaw, and Horseshoe Canyon formations in the south and east, (Gunther and Hills 1972; Jerzykiewicz and McLean 1980; Jerzykiewicz 1985*a*, 1997; Jerzykiewicz and Sweet 1988; Zubalich et al. 2021) and to the WF in northwest Alberta (Fanti et al. 2013; Zubalich et al. 2021) (Figs. 1 and 2). Despite this broad time equivalence, no radiometric dates or chronostratigraphic correlations have previously been determined for the Brazeau Formation. This study investigates the ashes and sedimentary deposits in outcrops that relate to dinosaur fossils (e.g., a bonebed, isolated specimens, footprints) in the area around Entrance, Alberta, which represent the upper portion of the "middle" Brazeau and limited isolated exposures of the "upper" Brazeau Formation (Lang 1947; Douglas and MacKay 1953; Jerzykiewicz 1985*b*; Dawson and Kalkreuth 1994). The interval of the Brazeau Formation that crops out near Entrance correlates to the upper units of each of the aforementioned formations surrounding the Brazeau Formation (Tolman and Carbon Mbr—HCF; Unit 4&5—WF; Upper St. Mary River facies—StMRF), which are all units that preserve few vertebrate remains compared to other units within their respective formations (Eberth et al. 2013; Eberth 2015; Voris et al. 2018; Fanti et al. 2022).

The Brazeau Formation outcrop investigated here lies within the western Upper Cretaceous Rocky Mountain foreland basin where subsidence and sedimentation rates would have been very high. Jerzykiewicz and Sweet (1988) proposed that the upper 50% of the formation (~500 of the 1000 m total thickness) is all Maastrichtian, based mainly on palynology. Interestingly, Eberth and Kamo (2020) propose that there was a significant reduction in sedimentation rate in the roughly time-equivalent Tolman Member of the HCF, which may correspond to an increase in subsidence in the foredeep further west and the corresponding capture of sediment there. In the present study, we report the first radiometric dates obtained for the Brazeau Formation and calculated sedimentation rates for the foothills region at this time (~70 Ma), which do indicate high rates of sediment deposition in the west. The new radiometric dates permit a refined correlation between the contact of the middle and upper Brazeau Formation to contact between the Tolman and Carbon members in the HCF.

This study presents new information for the chronostratigraphic, palaeobiogeographic, and palaeoecological distribution of *Edmontosaurus* from a new bonebed in the top of the middle Brazeau Formation from Entrance, Alberta. Although it was not possible to identify them to species level, two partial postorbitals represent important specimens for *Edmontosaurus* during the ~2.3 Myr temporal gap between *Edmontosaurus regalis* in Alberta and the Prince Creek Formation *Edmontosaurus* sp. in Alaska, and they expand the associated depositional palaeoenvironments associated with the genus into lake-margin settings.

Geological and palaeontological background

The Upper Cretaceous Brazeau Formation (Campanian–Maastrichtian) of the central foothills of Alberta represents a regression–transgression–regression succession that corresponds to the time-equivalent Belly River Group and HCF further east (Gunther and Hills 1972; Jerzykiewicz and McLean 1980; Jerzykiewicz 1985*a*, 1997; Jerzykiewicz and Sweet 1988; Gilbert et al. 2020; Zubalich et al. 2021) and to the WF further northwest (Fanti et al. 2013; Zubalich et al. 2021) (Figs. 1 and 2). The lower Brazeau Formation (Douglas 1958) is dominated by large channel sandstones and overbank mudstones representing landward deposits west of the "basal Belly River" deltas further east (e.g., Hamblin and Abrahamson 1996; Power and Walker 1996). Some of these sandstone packages closest to the Rocky Mountain front ranges contain conglomerates of variable thicknesses that thin eastward and are interpreted as evidence of braided rivers as they left the palaeo-Rocky Mountains rivers (Putnam 1993). The middle and upper Brazeau (Douglas 1958) intervals transition into a more proximal, upland setting with crevasse splay, lacustrine deposits, and paleosols (Jerzykiewicz and McLean 1980). Much of the formation underwent significant structural deformation during Eocene thrust faulting events (Pană and van der

Fig. 1. Lithological correlation of formations across central and northern Alberta. The figure is a combination of data from references listed at the top of each column.

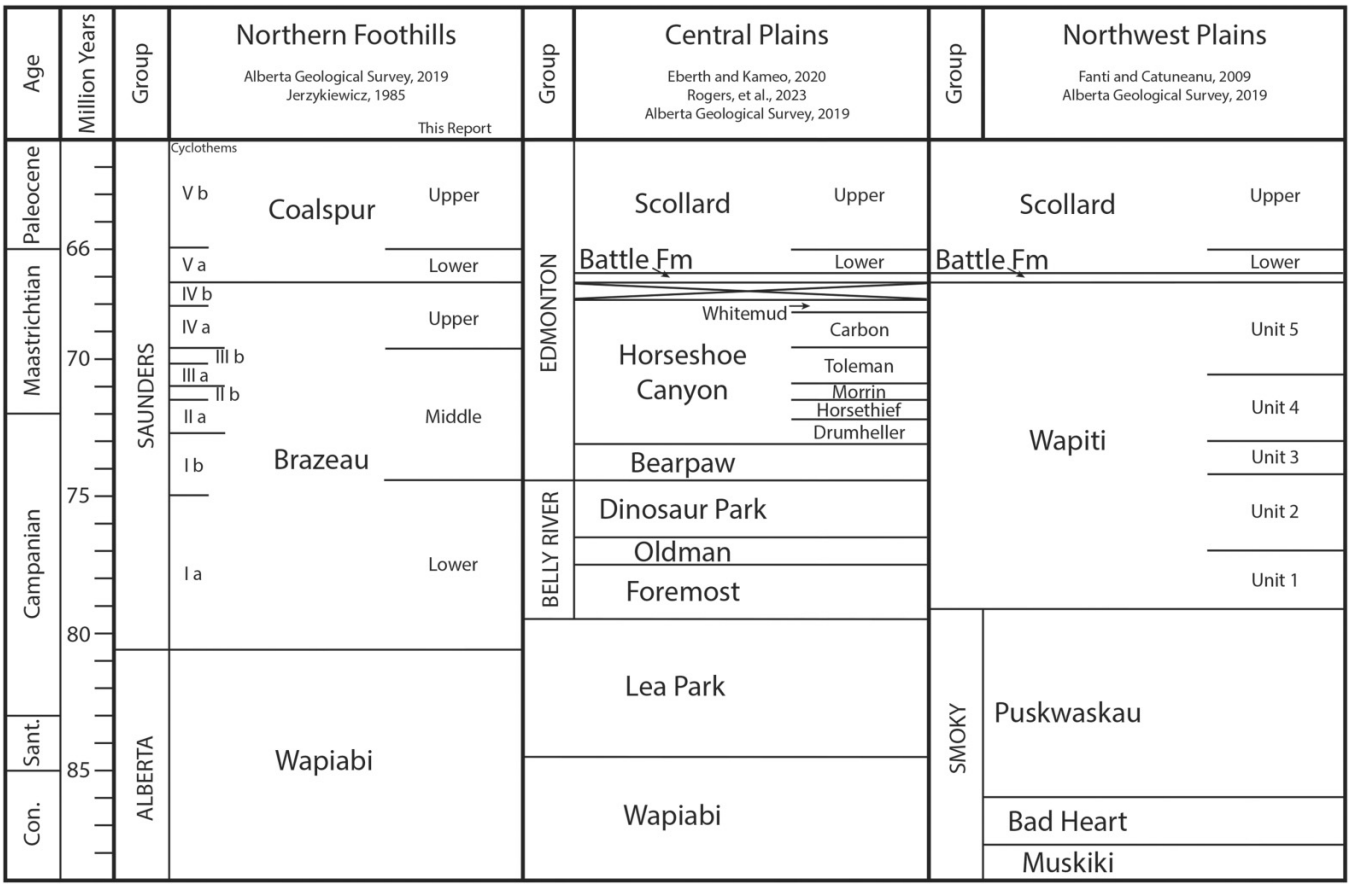

Pluijm 2014). Previous palynological work has provided relative dates for the correlation of the Brazeau Formation to other units within Alberta (Gunther and Hills 1972), but correlation between the Brazeau Formation other Alberta formations remains difficult with no previous radiometric dating.

Jerzykiewicz (1985*a*) provided a detailed summary of the Saunders Group sedimentology southeast of Hinton, Alberta. In his work, the Brazeau Formation was divided into four main cyclothems (Fig. 1), each consisting of two parts. Cyclothem I-a contains multiple large sandstones with chert pebbles at the base; Cyclothem I-b predominantly consists of overbank deposits with silicified tephras. Cyclothem II-a consists of several channel sandstones, whereas Cyclothem II-b was interpreted almost completely (88%) as overbank mudstones (Jerzykiewicz 1985*a*). Cyclothem III-a demonstrates an increase in channel sandstones (61.8%), and Cyclothem III-b preserves thin coal seams and significant overbank deposits (73.8%). The uppermost portion of the Brazeau Formation is formed by Cyclothem IV. Cyclothem IV-a is recognised by a distinct increase in thick (15 m) stacked sandstones, comprising nearly 74% of the section. Cyclothem IV-b returns to primarily overbank deposits (56%) with thin coaly mudstones and shales, coal beds, and bentonites. Jerzykiewicz (1985*a*) equated Cyclothem I-a to Douglas' (1958) lower Brazeau, Cyclothems I-b, II-ab, and III-ab to Douglas' middle Brazeau, and Cyclothem IV-ab to Douglas' upper Brazeau Formation. The area of study discussed herein is within Jerzykiewicz's (1985*a*) upper Cyclothem IIIb and IVa; however, for simplicity, Douglas' (1958) terminology of middle and upper Brazeau Formation is used instead.

Despite the poor chronology and complex stratigraphic correlation between outcrops generally within river cuts, the Brazeau Formation represents a largely uninterrupted terrestrial succession with no known significant unconformities, and provides an opportunity to investigate terrestrial ecosystems and vertebrate diversity during the Campanian and early Maastrichtian (Jerzykiewicz and McLean 1980). The bottom of the middle Brazeau interval, deposited during a regional transgression, is of particular interest because the correlative marine Bearpaw Formation (middle Campanian) preserves a limited nonmarine vertebrate fauna in southern Alberta from this time (Drysdale et al. 2018). However, the recovery of vertebrate remains from the Brazeau Formation is difficult due to forest cover and limited exposures that tend to be vertical cliff faces along swift-moving mountain rivers and streams. Consequently, little exploration has been conducted for palaeontological resources.

Before this study, the only reported Brazeau Formation vertebrates were tentatively identified as "*Gorgosaurus*" teeth and a "*Corythosaurus*" "toe bone" (Lang 1947). These specimens

Fig. 2. Map of southern Alberta formations that are equivalent to (at least in part) the Brazeau Formation. BpF, Bearpaw Formation; BRF, Blood River Formation; BRG, Belly River Group; DPF, Dinosaur Park Formation; EF, Eastend Formation; FF, Foremost Formation; HCF, Horseshoe Canyon Formation; SMRF, St. Mary River Formation; uBRF, upper Belly River Group; WF, Wapiti Formation. Summarized from AGS Map 600 (Prior et al. 2013).

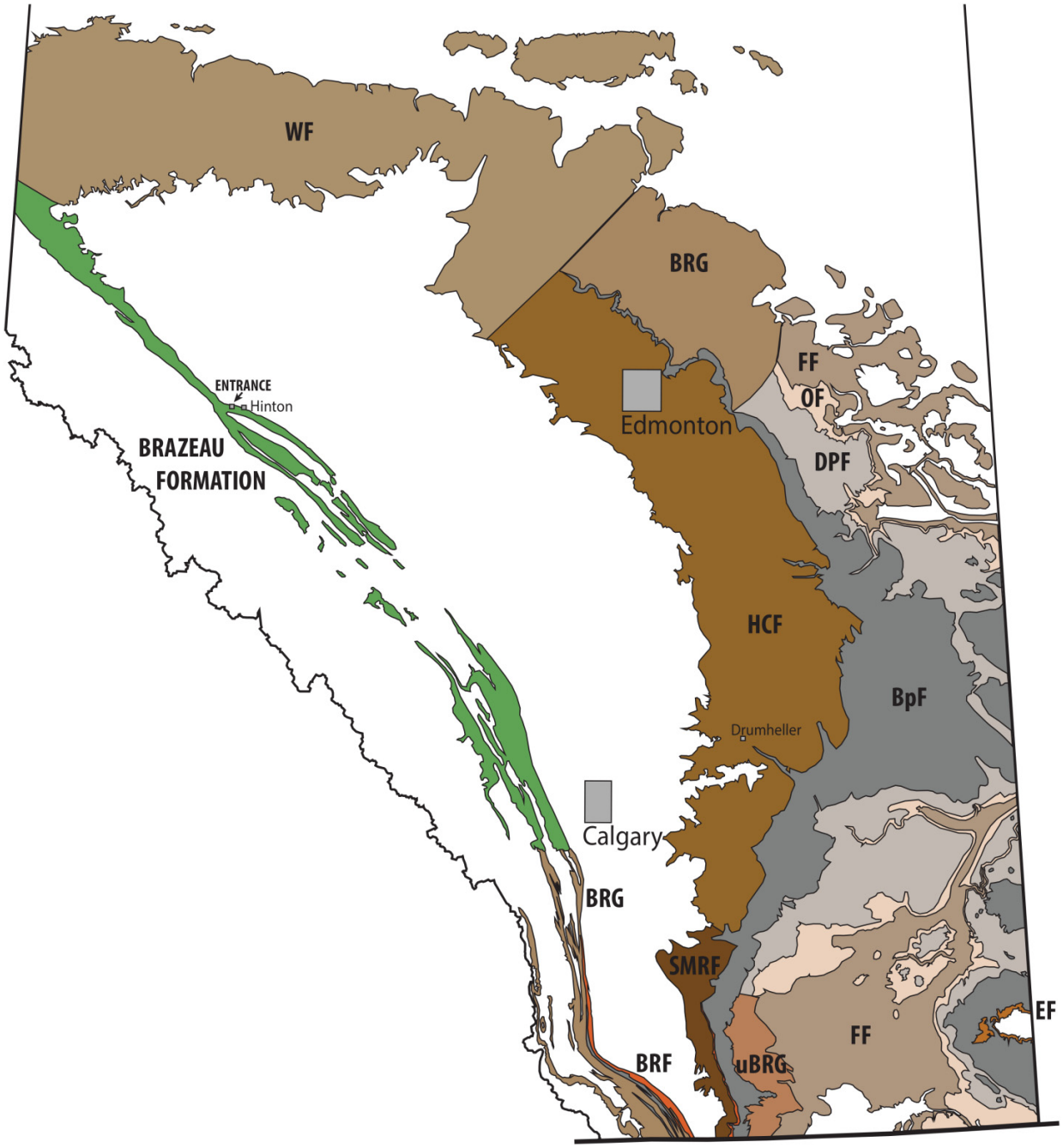

and several others were recovered from a railway rock cut (Fig. 3) in the early 1940s by R.C. Sibley, the local train station attendant in Entrance, Alberta, and sent to Barnum Brown at the American Museum of Natural History (AMNH) for identification. Barnum Brown, in his letters back to R.C. Sibley (Supplementary Material A), interpreted the specimens as likely originating from a bonebed; however, observations of the original mudstone layer from which the specimens originated suggest that the specimens were most likely from a single large disarticulated hadrosaur and associated tyrannosaur teeth. Investigation of this horizon indicates that there is no longer any of the Sibley fossil material exposed, nor were any new fossils found after digging into the layer in multiple positions. Additionally, the sizes of a tibia and a fibula recovered by Sibley indicate that they likely represent the same individual (Fig. 3). The Sibley specimens remain in New York and are now curated at the AMNH (FR 3838, FR 3839, FR 21608). In the late 1940s, R.C. Sibley delivered photographs of his spec-

Fig. 3. Photographs by R.C. Sibley to John Allan (Courtesy of EAS, U of A) of material collected in the 1940s along the abandoned Canadian Northern Railway. Specimens are now housed at the American Museum of Natural History (AMNH). (A) Horizon from which specimens were collected (white arrows marked by Sibley on original photographs). Note wooden railway ties at the base of exposure; ties are typically ~2.5 m long for scale. (B) Proximal hadrosaur humerus (left) and anterior portion of hadrosaur ilium missing preacetabular process (right) (AMNH FR 3839). (C) Large tibia (left) and large fibula (right) (AMNH FR 3839). (D) Variety of tyrannosaur teeth (AMNH FR 3838, FR 21608) and a large hadrosaur pedal ungual (far right).

Fig. 4. 1940s Sibley photograph (A) and modern photo (B) of the original and modern rock cut in comparison. Due to the expansion of the rock cut during the 1960s for highway construction, the topography of the hillside was altered such that the ground depression is now less visible. Expansion of the rock cut has also caused the apparent shift in the bedding position due to the intersection of the apparent bedding dip and the rock surface.

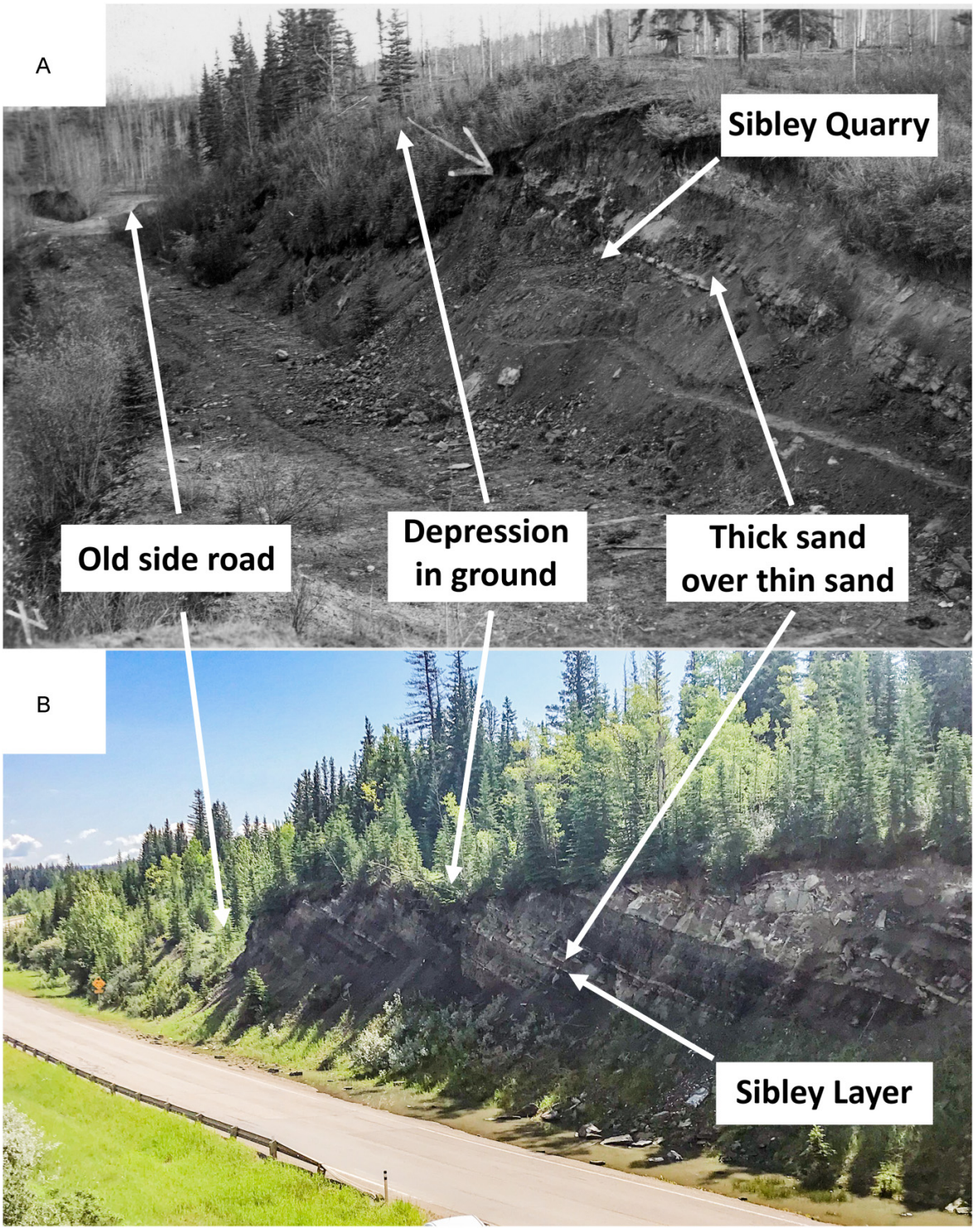

imens (Fig. 3) to Dr. John Allen at the University of Alberta to invite him to the site, an invitation he did not take. Unfortunately, during construction to convert the old rail line to a highway during the 1960s, the railway bed was expanded, and the Sibley site and any additional skeletal elements were destroyed. The photograph of the site R.C. Sibley provided to Dr. Allen was recently used to identify where the site would have originally been located (Fig. 4).

A second possible mention of vertebrate remains from the Brazeau Formation was published by Wann Langston (1959)

in the proceedings for the Ninth Annual Field Conference of the Canadian Society of Petroleum Geologists. Langston did not provide details except that the fauna in the "Saunders formation" (sic) is similar to that reported in the Foremost and Oldman formations with "*Myledaphus*, *Lepisosteus*, *Basilemys*, *Compsemys*, *Aspideretes*, a crocodile and various dinosaurs". The report of these taxa within the Brazeau Formation proper is questionable for multiple reasons. First, a thorough search of museum collections where these vertebrate remains may have been accessioned (AMNH, British Museum of Natural History, Canadian Museum of Nature (CMN), McGill University, Royal Ontario Museum (ROM), Royal Tyrrell Museum, Royal Saskatchewan Museum (RSM), Texas Science and Natural History Museum, University of Alberta, and the University of Saskatchewan) indicated that there were no specimens collected, except for dinosaurs, by the time Langston published his field trip guide. Similarly, no records of *Aspideretes*, *Basilemys*, *Compsemys*, *Lepistosteus*, or *Myledaphus* are known from the Brazeau Formation in any repository database. Secondly, the "Saunders formation", now the Saunders Group, consists of the (oldest to youngest) Brazeau, Coalspur, and Paskapoo formations, with the Brazeau grading into the Belly River Group (Drywood Creek, Lundbrook Creek, and Connelly Creek formations) in the southern foothills of the area that Langston (1959) described for his field guide. Museum collection searches do indicate that each of the taxa listed by Langston have had representative specimens recovered from the Belly River Group, which is time-equivalent to the lower half of the Brazeau Formation. Additionally, microvertebrate sites are very difficult to find in the Brazeau Formation due to the well-cemented nature of the sandstones, which generally prevent sufficient weathering to appropriately expose the small elements from fish and turtles, such as those reported by Langston (1959). For these reasons, it is plausible that Wann Langston (1959) confused the northern extent of the Belly River Group with that of the Brazeau Formation. As such, this project rejects the identification of the taxa that Wann Langston (1959) lists in his field guide as originating from the Brazeau Formation, and further investigation into the formation is required to confirm their presence.

In 2017, a rumoured bonebed in Entrance, Alberta (8.5 km west of Hinton) (Fig. 5) was investigated. Test-pit excavation of the Bennett Bonebed, named after the landowner at the time, began in August 2018. The bonebed was initially exposed in the late 1970s during the construction of a driveway on the property and lay ~24 m stratigraphically below the specimens R.C. Sibley recovered in the 1940s. Work in 2018 and 2019 recovered 126 specimens from three-quarters of a square metre, including a well-preserved juvenile hadrosaur left postorbital (University of Alberta Laboratory for Vertebrate Palaeontology (UALVP) 59617) and a subadult right postorbital fragment (UALVP 60423) identified as *Edmontosaurus* sp. With such an abundance of specimens collected from such a small area and the lack of vertebrate remains otherwise known from the Brazeau Formation, the Bennett Bonebed could provide important information into lower-middle Maastrichtian palaeo-Rocky Mountain foothill ecosystems. In addition, eight volcanogenic beds in close stratigraphic association with the bonebed were sampled for zircon U–Pb geochronology, yielding the first radiometric dates for the Brazeau Formation. The discovery of *Edmontosaurus* sp. at the Bennett Bonebed now expands the distribution of this genus to the Brazeau Formation, HCF, SMRF, and WF in Alberta (Lambe 1920; Eberth et al. 2013; Bell and Campione 2014; Bell et al. 2014; Evans et al. 2015; Campbell et al. 2020). Additionally, a sandstone bed that overlays the Sibley layer contains casts of several hadrosaur footprints on the bottom side as infill casts, which are the first fossil footprints reported from the Brazeau Formation.

This paper describes the two partial *Edmontosaurus* postorbitals and a large hadrosaur footprint from the top of the middle Brazeau Formation. The depositional setting of the stratigraphic section through and above the Bennett Bonebed is interpreted based on detailed sedimentology from the lower ~60 m of the stratigraphic section presented here. The tephra dates reported here are used to develop an age model that spans the top of the middle and the bottom of the upper Brazeau Formation from the ~263 m of strata exposed. Sedimentation rates are calculated and are discussed in terms of the subsidence of the Alberta foreland basin depocenter, as well as their importance for interpreting a more regional view of time-equivalent units further east (i.e., Tolman and Carbon members of the HCF).

Materials and methods

Excavation and preparation

The Bennett Bonebed is located on private property west of Hinton, Alberta. The site was excavated using jackhammer and hand tools (e.g., hammer, chisel, and awls). Due to the unpredictability of fracturing in the hard encasing mudstone in such a high bone density area, elements were stabilized using Paraloid and let dry before removal. The bonebed was mapped using a grid system along a baseline to the centre of the bone and drawn into 1×1 m^2 that represented a specific square meter in the test pit. Specimens that were heavily permineralized were removed from the matrix in parts or whole, wrapped in paper towel, and placed into a plastic baggie. Specimens that were poorly permineralized received several doses of Paraloid and were removed from the bonebed with matrix still surrounding them, either wrapped in paper towels or in small plaster and cheesecloth jackets. Once the specimens were in the laboratory, they were prepared using small pneumatic air scribes after any cracks or break surfaces were consolidated with Paraloid and glued with medium viscosity cyanoacrylate. The specimens are now accessioned at the UALVP.

Specimen imaging

UALVP specimen photographs were taken using a Canon 7D Mark II with a Tamron 24–70 mm lens set to 70 mm with ISO 100, f/6.3, and 1/250 exposure time. Two Canon Speedlite 600EX flashes were set at 180° to illuminate the specimen evenly. Three-dimensional models of UALVP 59617 (juvenile postorbital) were created using FlexScan3D V 3.3.9.1 software with a Polyga HDI Advance R5X-Monochrome 3D Scanner. Three-dimensional models of UALVP 60423 (subadult postor-

Fig. 5. Geological map of the area surrounding the Bennett Bonebed showing formations and geological structures. Dates are the approximate ages of corresponding thrust faults (Pană and van der Pluijm 2014). Modified from Alberta Geological Survey Map 560 (Pană and Elgr 2013).

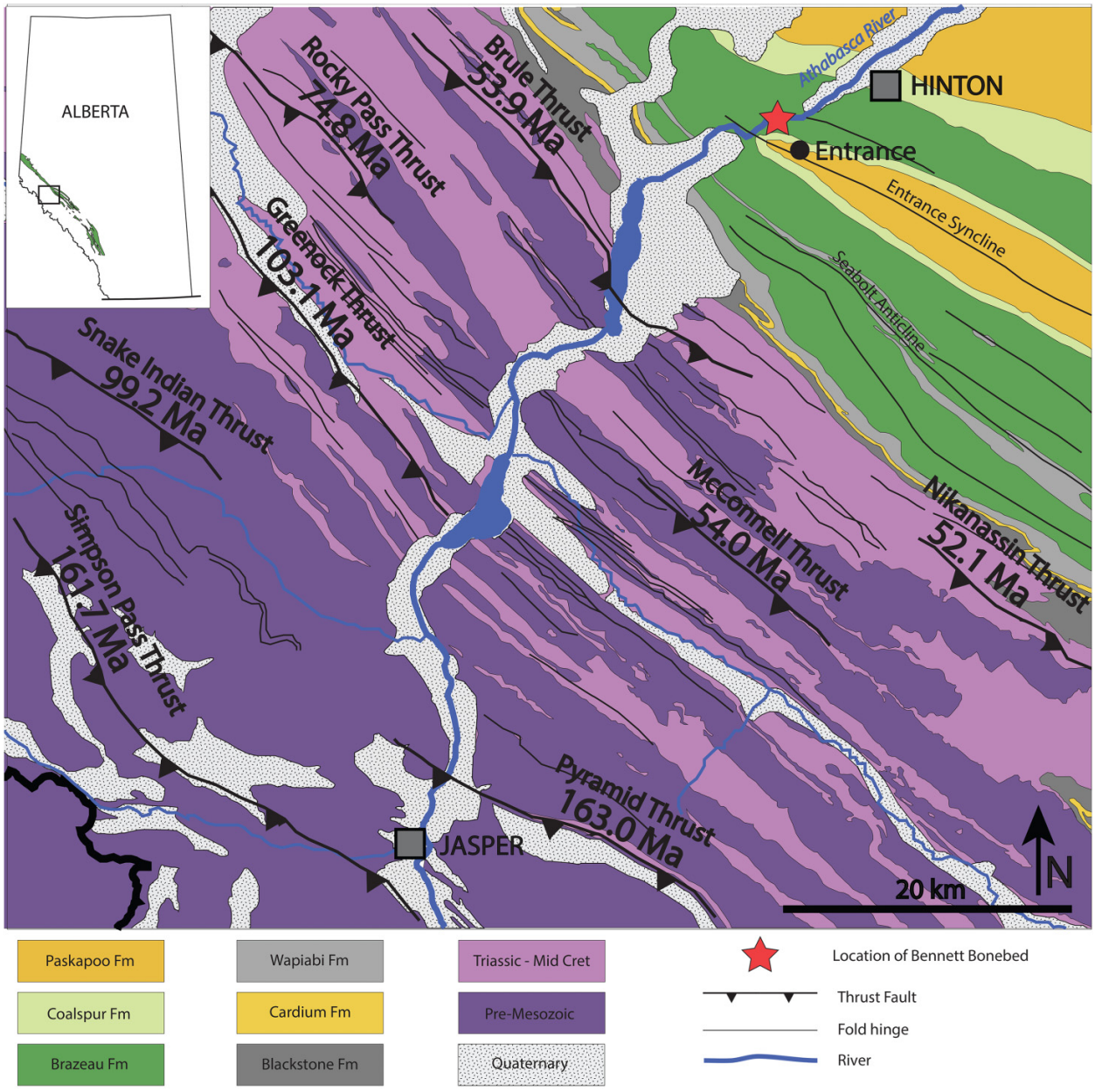

bital fragment) were created using 133 images in Agisoft Metashape Professional photogrammetric software. Models of both specimens shown here were manipulated in the ORS software Dragonfly 3.6.

Stratigraphy and sedimentology

Stratigraphic thicknesses from 0 to 61 m were obtained using a Jacob's staff with Abney level. Sediments were observed along the complete measured thickness where data were recorded. Grain size, sedimentary structures, and other sedimentary features (e.g., root marks), estimated mud content, rock colour, and bed contacts were recorded throughout at centimetre-scale resolution for the lower 62 m of section. The upper part of the exposed road-cut section and the Athabasca River section (higher than 61 m) have not yet been logged, but thicknesses and stratigraphic position of the uppermost tephra was extrapolated using an orthographic image of the outcrop (methods below). Two sections were measured. The first was along the private driveway on which the bonebed is exposed, from 0 to 22.5 m, and the second and longer section is located along Hwy 40 across from the driveway section, from 17 to 62 m (with ~6.5 m overlap between the sections).

Correlation of the two sections (driveway and Hwy 40) was performed using a Nikon XS 3″ reflectorless total station to sight a base of a sandstone at 22 m. The total station was oriented directly north and calibrated using a TRC5 handheld

Fig. 6. Weighted average plots for zircons isolated from their respective tephra layer. Each bar represents a single zircon; blue bars are outliers.

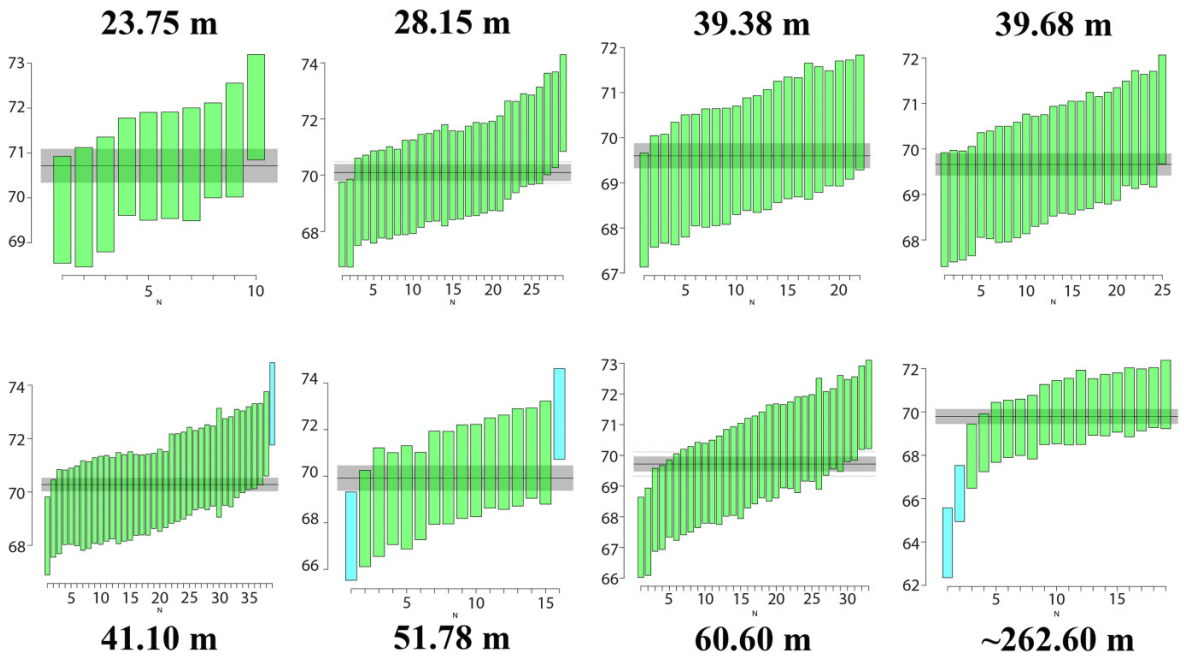

control device. The total station was then rotated to the local strike of 104°E, with the crosshairs falling ~15 cm above the base of a 50 cm thick sandstone. To estimate the stratigraphic elevation above the bonebed for unmeasured positions (e.g., middle-upper Brazeau contact, 262.6 m tephra), a GPS-calibrated 3D map of the area was produced using a DJI Mavic Pro Platinum aerial drone 4K video imported into Agisoft Metashape Professional. Once the 3D model was created, the model was rotated digitally to orient it to the dip direction (194°E), then tilted back to horizontal (34°) to correct for dip (and apparent dip). Once the model was oriented correctly, an orthographic image was made to remove all visual distortion due to changes in perspective. Horizontal and vertical distances from the centre of the 60.60 m ash up to the middle-upper Brazeau contact and the ~262.60 m ash were then calculated by Metashape on the orthographic image. The vertical distances calculated for the positions of interest were then added to the 60.60 m, providing an estimated stratigraphic position above the base of the measured section.

Geological maps of the region (Lang 1947; Pana and Elgr 2013; Prior et al. 2013) indicate that no major change in dip occurs between the bonebed and the ~262.60 m ash, and neither are there any known faults. Therefore, calculated depositional rates based on total thickness of the section around the Bennett Bonebed is considered to not have been influenced by tectonic processes during thrust faulting in the immediate area.

Tephra geochronology and Bayesian age model

Nine tephra deposits were found between 23.75 and ~262.6 m stratigraphically above the Bennett Bonebed, eight of which were dated (Figs. 6 and 7). An erosional contact overlain by mudstone cut into the 28.15 m tephra; however, the preserved ash pockets were only slightly disturbed, and zircon dates were coherent, indicating that no significant contamination occurred. The remaining tephras (23.75, 39.38, 39.68, 41.10, 51.78, 60.60, and ~262.60 m) are between 15 and 60 cm thick, in planar continuous beds that are uniform in thickness. The tephras each infill (drape) low-relief undulations in underlying beds, have sharp lower and upper contacts, and are very light yellow in colour with no apparent mixing of other sediments observed, which indicates that the tephras are intact and have not been contaminated by reworked sediments. Large (~2 kg) samples were collected from the centre of each bed for zircon U–Pb geochronology to constrain the timing of the eruption associated with each tephra. These samples were collected from the centre of each tephra to ensure that no groundwater or ancient plant-rooting transported contaminations into the upper or lower surfaces of the ash. A Bayesian age model for the local stratigraphic section was produced (methods below) to approximate the depositional age of the Bennett Bonebed, Sibley layer, footprint bed, and the middle/upper Brazeau Formation contact.

Each tephra sample was fluidized into a slurry in water and passed across a Wilfley table to concentrate dense minerals, similar to the method described by Söderlund and Johansson (2002). Great care was taken to clean the Wilfley table between each sample to reduce the risk of contamination. From the dense mineral concentrate, ~50–100 zircons were hand-picked to mount in epoxy. The grain mount was polished to expose the grain centres, and regions suitable for analysis were identified from cathodoluminescence imaging.

U–Pb zircon data (Supplementary Material B) were collected using laser ablation multicollector inductively coupled mass spectrometry (LA-MC-ICPMS) at the Canadian Centre for

Fig. 7. Volcanoclastic dates and relative positions above the Bennett Bonebed (orthographs are not to scale with each other). (A) Orthographic image of Bennett Bonebed and surrounding exposure produced to remove modern dip angle, restoring bedding back to original horizontal position. Roadcut tephras are labelled with their corresponding stratigraphic position above the bonebed and radiometric dates. The layer from which R.C. Sibley collected his specimens and trackway layer are indicated. (B) Orthographic image of the east bank of the Athabasca River and the uppermost portion of the studied outcrop indicating where the middle and upper Brazeau Formation contact and ~262.60 m tephra lies. (C) Satellite image of each outcrop section. The red line indicates the road section in "A", and the yellow line indicates the Athabasca River section in "B". Note the overlap between the two sections where the 60.60 m tephra is located in both orthographs.

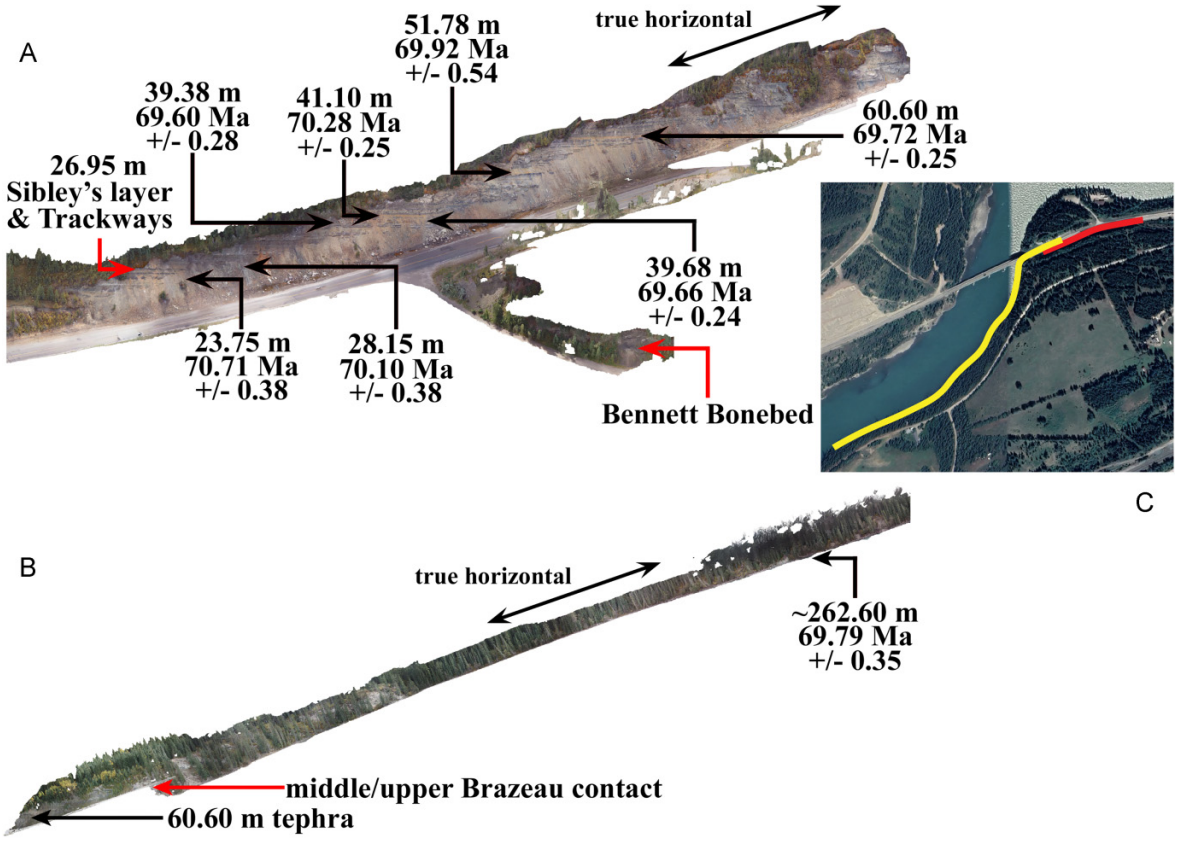

Isotopic Microanalysis at the University of Alberta, Edmonton, Canada, using procedures modified from Simonetti et al. (2005). The analytical setup consists of a New Wave UP-213 LA system interfaced with a Nu Plasma MC-ICPMS equipped with three ion counters and 12 Faraday cups. We operated the laser at 4 Hz with a beam diameter of 30 μm, which yielded a fluence of ~1–3 J/cm^2. Ablations were conducted in a He atmosphere at a flow rate of 1 L/min through the ablation cell. Output from the cell was joined to the output from a standard Nu Plasma desolvating nebulizer (DSN). On-peak gas + acid blanks (30 s) were measured prior to a set of analyses. Data were collected statically, consisting of 30 1 s integrations. Before and after each set of analyses, zircon reference materials GJ1 (Jackson et al. 2004), Plesovice (Sláma et al. 2008), and 9435 (Klepeis et al. 1998) standards were repeatedly analysed to monitor U–Pb fractionation, reproducibility, instrument drift, and to assess data quality. Mass bias for Pb isotopes was corrected by measuring ^{205}Tl/^{203}Tl from an aspirated Tl solution (NIST SRM 997) via the DSN-100 DSN using an exponential mass fractionation law and assuming a natural ^{205}Tl/^{203}Tl of 2.3871. All data were reduced offline using an Excel-based program. Unknowns were normalized to GJ1 as the primary reference; Plesovice and 9435 were treated as unknowns to assess data quality and yielded weighted average ^{206}Pb/^{238}U dates of 336.4 ± 1.4 Ma 95% confidence (n = 29/33, MSWD = 1.1), and 55.52 ± 0.22 95% confidence (n = 32/33, MSWD = 1.5) within uncertainty of reported dates. The uncertainties reported on individual data points are a quadratic combination of the internal measurement precision and the overall reproducibility of the standards during an analytical session ~1% for ^{207}Pb/^{206}Pb, and ~2% for ^{206}Pb/^{238}U, 2 s. The long-term excess scatter in ^{206}Pb/^{238}U sessional weighted means, beyond weighted mean errors for Plesovice is 0.48% (2 s), which is propagated into the weighted mean errors for this study, shown in brackets in the results. The data are corrected for common Pb using a ^{207}Pb-based approach due to the difficulty of resolving transient contributions of ^{204}Hg present in the Ar gas from ^{204}Pb present in either the crystal and/or the acid + gas blank. Thus, reported ^{204}Pb values are for informational purposes only but can be useful for identifying and rejecting samples that have obviously large amounts of common Pb.

Quoted ages for each tephra are the 2σ error-weighted mean of the youngest coherent population of $^{206}Pb/^{238}U$ zircon dates (propagated excess scatter shown in brackets), calculated using the *weighted mean* function, with outlier detection, in the *IsoplotR* package within the R software environment (Vermeesch 2018) (Fig. 6). A Bayesian age-depth model was then calculated using the R package *Bchron* (Haslett and Parnell 2008) (Supplementary Material C) and the 2σ error-weighted mean ages for the tephra (Fig. 8; Supplementary Materials D and E). *Bchron* uses prior knowledge (i.e., constraints from stratigraphic superposition and the requirement for positive sedimentation rates) to iteratively construct plausible age-depth models with quantified uncertainty, based on dated beds. Alternative age models model using the 0.48% error from the 9435 reference (Fig. 8; Supplementary Materials D and F) or the 1% error from the Plesovice reference (Supplementary Materials C and G) do not alter our conclusions. All quoted ages for the Sibley layer, trackway layer, Bennett Bonebed, and middle/upper Brazeau Formation contacts were obtained from the *Bchron* age model.

Monte Carlo simulation was used to calculate the range of plausible sedimentation rates between the uppermost and lowermost dated tephra based on the *Bchron* age model. Normal distributions for the modeled ages were defined at the 23.75 and ~262.6 m tephra, then we iteratively calculated 10 000 sedimentation rates based on random draws from those age probability distributions. In turn, the median sedimentation rate and associated 1σ/2σ uncertainty (0.34–0.68 and 0.025–0.975 quantiles, respectively) were drawn from the 10 000 iteratively calculated sedimentation rates.

Institutional abbreviations

AMNH—American Museum of Natural History, New York, USA; **CMN**—Canadian Museum of Nature, Ottawa, Canada; **ROM**—Royal Ontario Museum, Toronto, Canada; **RSM**—Royal Saskatchewan Museum, Regina, Canada; **UALVP**—University of Alberta Laboratory for Vertebrate Palaeontology, Edmonton, Canada; **UAMES**—University of Alaska Museum, Fairbanks, USA.

Locality

The Bennett Bonebed is located on private property near Entrance, Alberta. As per the property owners' requests, the specific location of the bonebed is not included here. GPS information for the bonebed site and tephra collection sites can be obtained through the UALVP for researchers and research purposes only. Quarry maps will be published in a more thorough description and analysis of the bonebed when a more expanded excavation has been conducted.

The exact position of the R.C. Sibley site is impossible to determine due to the site having been destroyed during highway expansion. However, the original dig site is estimated to have been at approximately 453 895 mE; 5914 597 mN (UTM 11U), and ~3 m above the current highway grade. The modern position of the Sibley layer crops out at 453 909 mE; 5914 590 mN.

Results

Description and comparison

Skeletal remains

The hadrosaur postorbital UALVP 59617 is well preserved and is approximately 75% complete, but it is missing most of the jugal process and the most posterior centimetre of the squamosal process (Fig. 9). The preserved portion of the fossil has an anteroposterior length of 123 mm and a mediolateral width of 73 mm. The specimen is most similar to the postorbital of the holotype (CMN 2288) and paratype (CMN 2289) of *Edmontosaurus regalis* (Lambe 1920; Campione and Evans 2011; Xing et al. 2017) (Fig. 10). It is also similar to the postorbital of a juvenile *Edmontosaurus regalis* (UALVP 60425; Fig. 10) from the Horseshoe Canon Formation. The anteriorly oriented frontal process is triangular with a frontal contact surface that possesses two anteroposteriorly oriented grooves. Unfortunately, the ridge that forms the dorsal margin of the top groove is missing, so the complete depth is unknown. The lower, much larger groove extends the entire length of the frontal contact and forms approximately 80% of the height of the contact surface. The anteromedial process is similar to those in CMN 2288 and CMN 2289 but differs slightly in that it hooks posteriorly. In contrast, the anteromedial process in the juvenile, UALVP 60425, is narrow and elongated medially. The anteromedial process of UALVP 59617 preserves a tripartite contact with three thin, tall ridges for a limited contact surface with the parietal. Although missing the most distal edge, the squamosal process is a thin, lateroventrally dipping, bladelike structure that extends posteriorly with a slight medial deflection. The medial surface has a slightly rippled texture for the contact with the squamosal. This resembles the orientation of the process observed on *Edmontosaurus regalis* (CMN 2288, 2289) and differs from *Edmontosaurus annectens* (CMN 8509, ROM 64076, RSM P3234.1.1), in which the process is oriented such that the "blade" is more vertical, causing a narrow appearance in dorsal view.

The main body of the postorbital is well preserved and possesses a large laterosphenoid fossa oriented medially and located directly ventral to the anteromedial process. The dorsolateral surface is expanded due to the development of an enlarged postorbital fossa along the orbit edge. The presence of the postorbital fossa is a diagnostic character for the genus *Edmontosaurus* (Campione and Evans 2011; Xing et al. 2017). The postorbital fossa of UALVP 59617 is large for the size of the postorbital and similar in size to that of the pocket in the Alaskan Prince Creek Formation *Edmontosaurus* sp. postorbital UAMES 33308 (Mori et al. 2016; Xing et al. 2017; Takasaki et al. 2020), where the pocket is relatively wider than in similarly sized *Edmontosaurus annectens* (Takasaki et al. 2020). Although histological sections have not been conducted for either specimen, UALVP 59617 is interpreted as representing a juvenile/subadult individual based on the size discrepancy between it and UALVP 60423.

UALVP 60423 (Fig. 11) is a fragment of a right postorbital preserving a partial squamosal process with postorbital fossa from a subadult individual. Due to the incomplete nature of

Fig. 8. Measured section of the bonebed section (left) and the Hwy 40 section (right) with U–Pb geochronology and Bchron Bayesian age model results correlated with the full section.

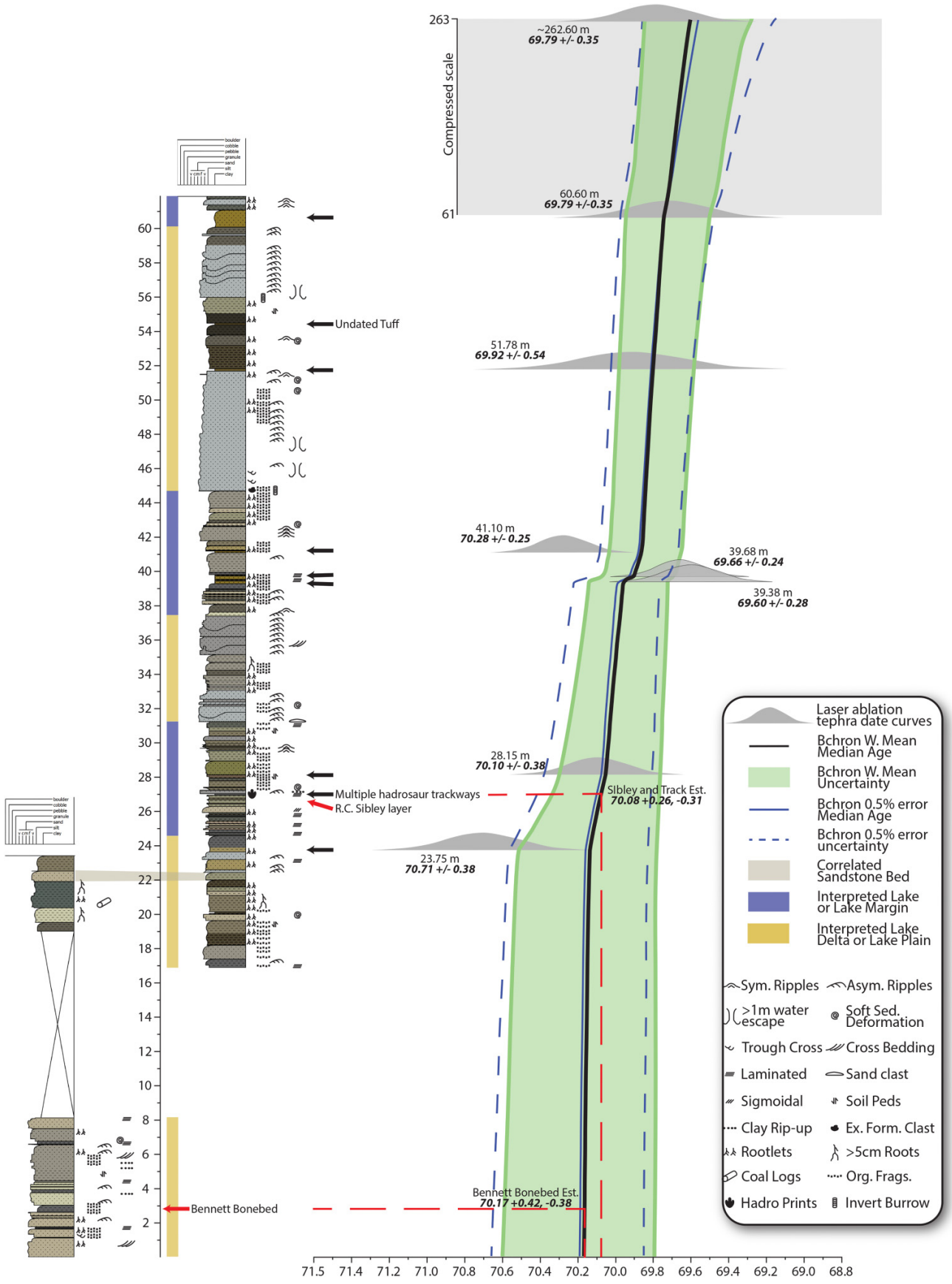

Fig. 9. UALVP 59617, *Edmontosaurus* sp. left postorbital. Corresponding letters represent the same view. Capital letters are photographs and lower-case letters are 3D models. (A) Dorsal view. (B) Ventral view. (C) Lateral view. (D) Medial view. (E) Anterior view. (F) Posterior view. Abbreviations: amp, anteromedial process; fp, frontal process; lsp, laterosphenoid fossa; pof, postorbital fossa; sp, squamosal process. Black arrows indicate anterior.

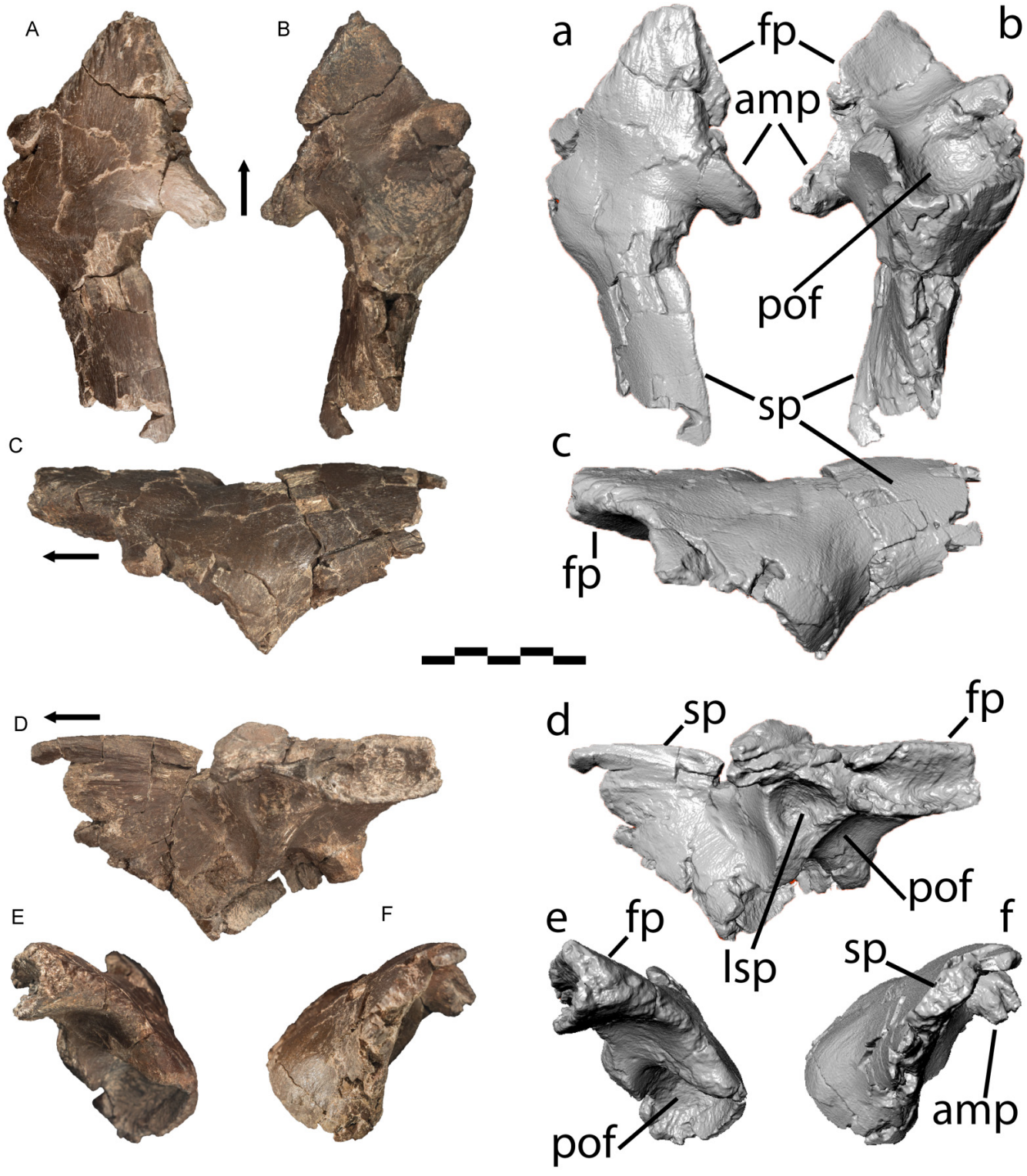

the specimen, no meaningful measurements can be taken. The squamosal process preserves the rugose surface of the ventral squamosal contact; however, the most posterior edge of the process is missing. The medial third of the squamosal process is also missing (Fig. 11). Anterior to the squamosal process, the postorbital fossa expands dorsally and laterally,

Fig. 10. Postorbital outlines of *Edmontosaurus*. (A) *Edmontosaurus regalis* (holotype, CMN 2288) left postorbital in dorsal (left) and lateral (right) views. (B) *Edmontosaurus regalis* (paratype, CMN 2289) left postorbital in dorsal (left) and lateral (right) views. (C) *Edmontosaurus* sp. (UALVP 59617) left postorbital in dorsal (left) and lateral (right) views. (D) *Edmontosaurus regalis* (UALVP 60425) left postorbital in dorsal (left) and lateral (right) views. (E) *Edmontosaurus annectens* (CMN 8509) left postorbital in dorsal (left) and lateral (right) views. (F) *Edmontosaurus annectens* (RSM P3234.1.1) right postorbital (reflected) in dorsal (left) and lateral (right) views. (G) *Edmontosaurus annectens* (ROM 64076) right postorbital (reflected) in dorsal (left) and lateral (right) views. Scale bar is 5 cm.

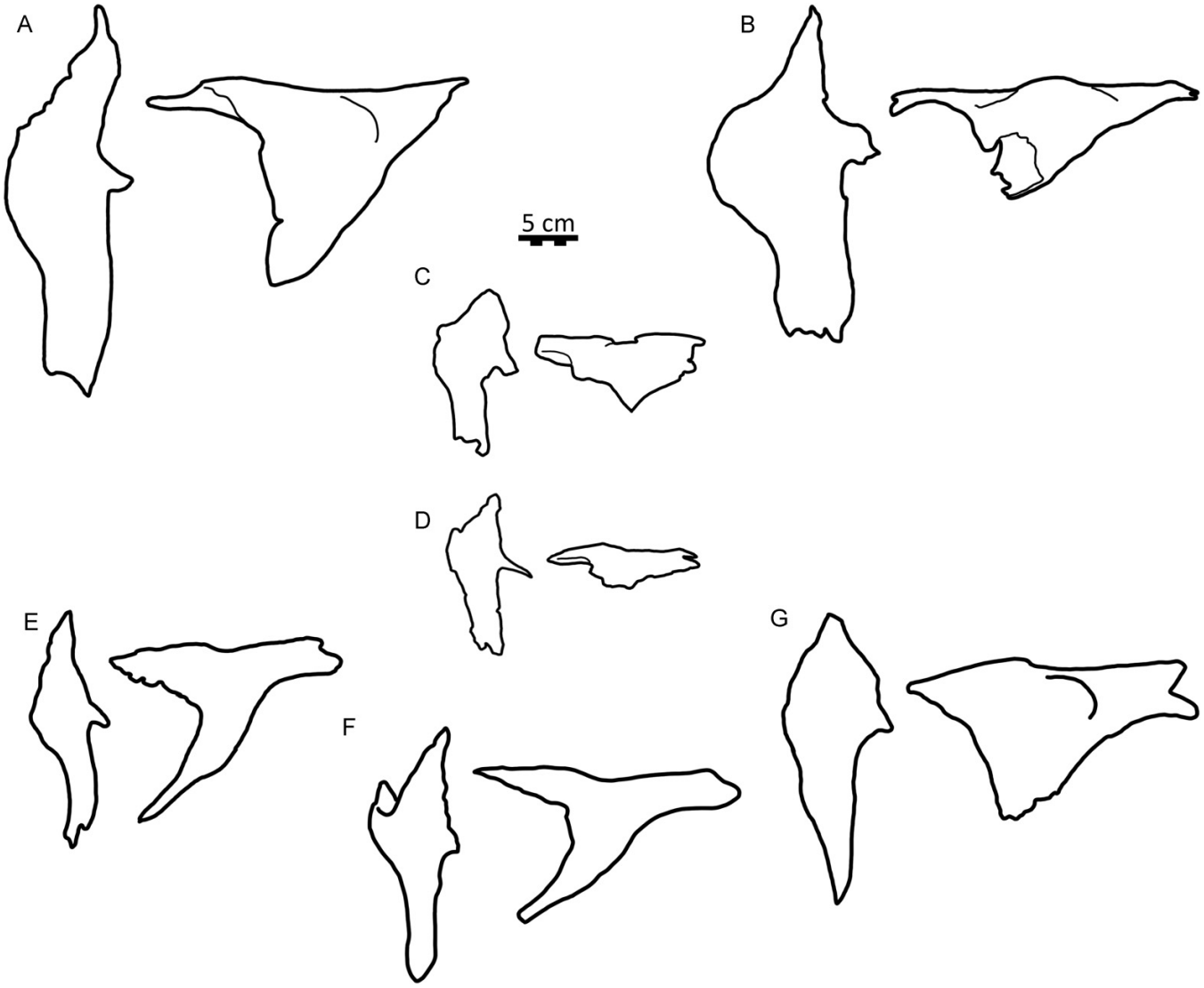

indicating that the fossa would have been quite enlarged if complete.

Footprints

The thinly laminated, dark grey mudstone layer of the Sibley layer is overlain by a well-cemented sandstone with mudstone clasts in the base. The sandstone-filled depressions on the upper mudstone surface represent four dinosaur footprints, one clear and three vague, all of which are only partially exposed on the bottom of the sandstone bed. The footprints are preserved as sandstone casts that infill footprint depressions in wet mud. They are now exposed on the bottom of a dipping sandstone bed, visible due to the road cut.

The best-preserved footprint cast was photographed, but specimens were not collected due to the instability of the outcrop (Fig. 12). Digit III pad measures ~32 cm long, and digit II pad is ~30 cm long. The visible digits are both broad and terminate at a rounded end. The print possesses long, shallow striae aligned with the length of each digit that may have formed by scale drags when the animal pulled its foot out of the mud. The foot pad and digit II are contained within the road cut and are not visible. The cast represents a large pes print, tentatively assigned to *Hadrosauropodus* isp. (Lockley et al. 2004), based on digit morphology and its close resemblance to footprints assigned to the ichnogenus preserved in the WF (Fanti et al. 2013; McCrea et al. 2014).

Fig. 11. UALVP 60403. Corresponding letters represent the same view. Capital letters are photographs and lower-case letters are 3D models. (A) Dorsal view. (B) Ventral view. (C) Lateral view. (D) Medial view. (E) Anterior view. (F) Posterior view. Postorbital fragment superimposed on CMN 2289 to show its original position in Dorsal view (G) and lateral view (H) (not to scale). Abbreviations: fr, frontal; po, postorbital; pof, postorbital fossa; sq, squamosal. Scale bar is 5 cm.

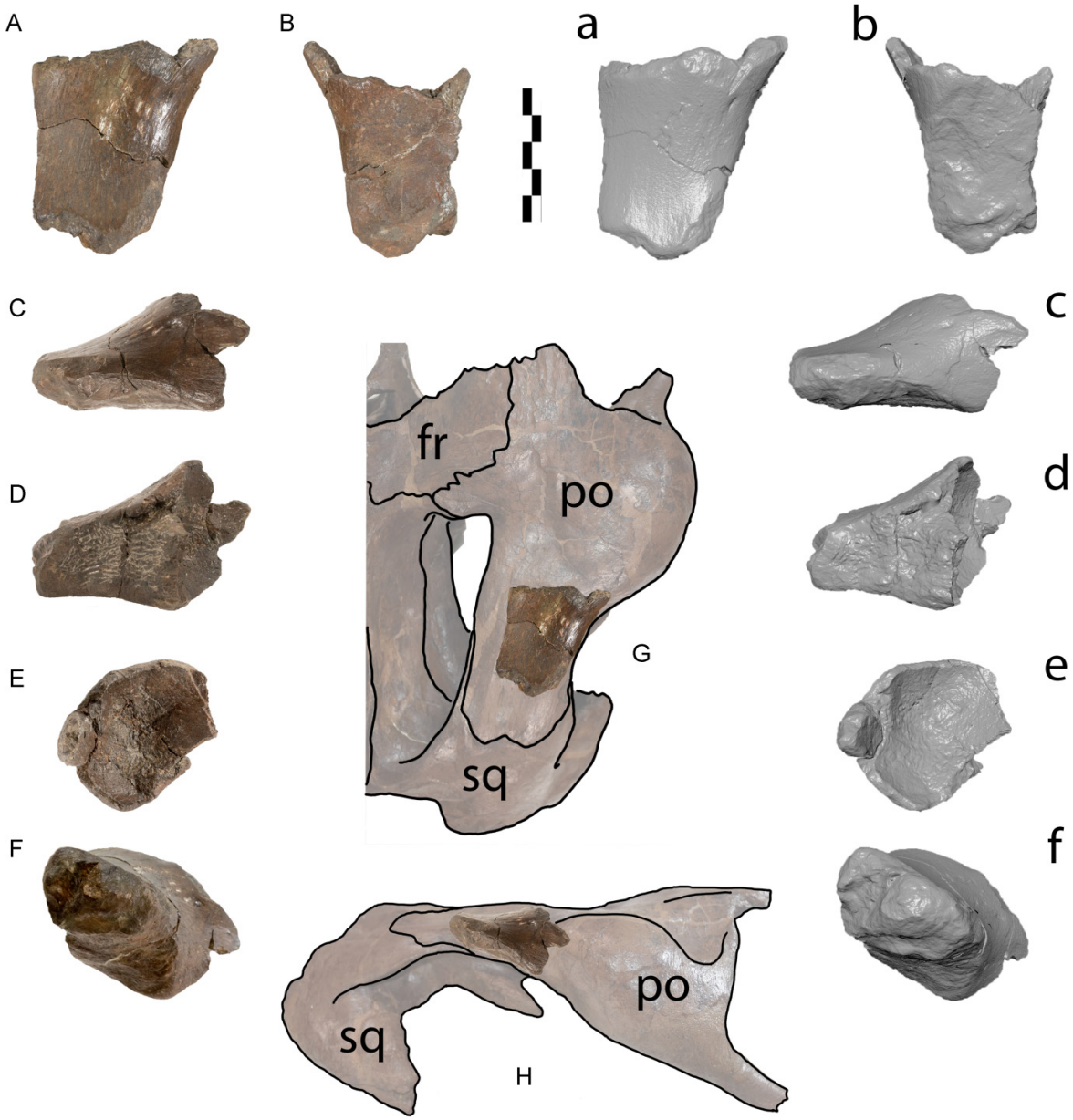

Depositional setting

Lithology, sedimentary structures, and bed geometry for the bonebed and overlying strata were studied to interpret the depositional environment. The surrounding bonebed matrix is siltstone with rare, flattened claystone clasts up to 2 cm in diameter. Within the bonebed, vertebrate specimens appear to be sorted by size, decreasing in size upwards. Four multidecimetre (20–50 cm thick) current-rippled sandstone and horizontal laminated sandstone/mudstone heterolithic beds overlay the bonebed. A large sedimentary structure, interpreted as a sandstone pillow within a laminated mudstone 1 m above the bonebed (Fig. 13A), indicates rapid deposition of sand into water-saturated or submerged sediments, representing a subaqueous setting for the bonebed.

The 45 m long section of outcrop along Highway 40 (~70 m SE of the bonebed) exhibits repeated 1–2 m coarsening-upward packages from siltstone to fine-grained sandstone (Fig. 8). The number of thin (2–5 cm), planar sandstone beds progressively increase upward in the section with each subsequent coarsening-upward package, along with laminated siltstone and mudstone (Fig. 13B). Partially chert-cemented interbedded siltstone (lower) and very fine-grained (lower) sandstone with wave-ripple cross lamination (Figs. 13B and 13C) are present ~27 m above the bonebed. These interbedded deposits are covered by a 10 cm thick wave-rippled fine-grained

Fig. 12. Natural sandstone cast of cf. *Hadrosauropodus* isp. in situ exposed along the Hwy 40 rock cut. Bottom: Line drawing highlighting the overall shape and drag marks on the surface.

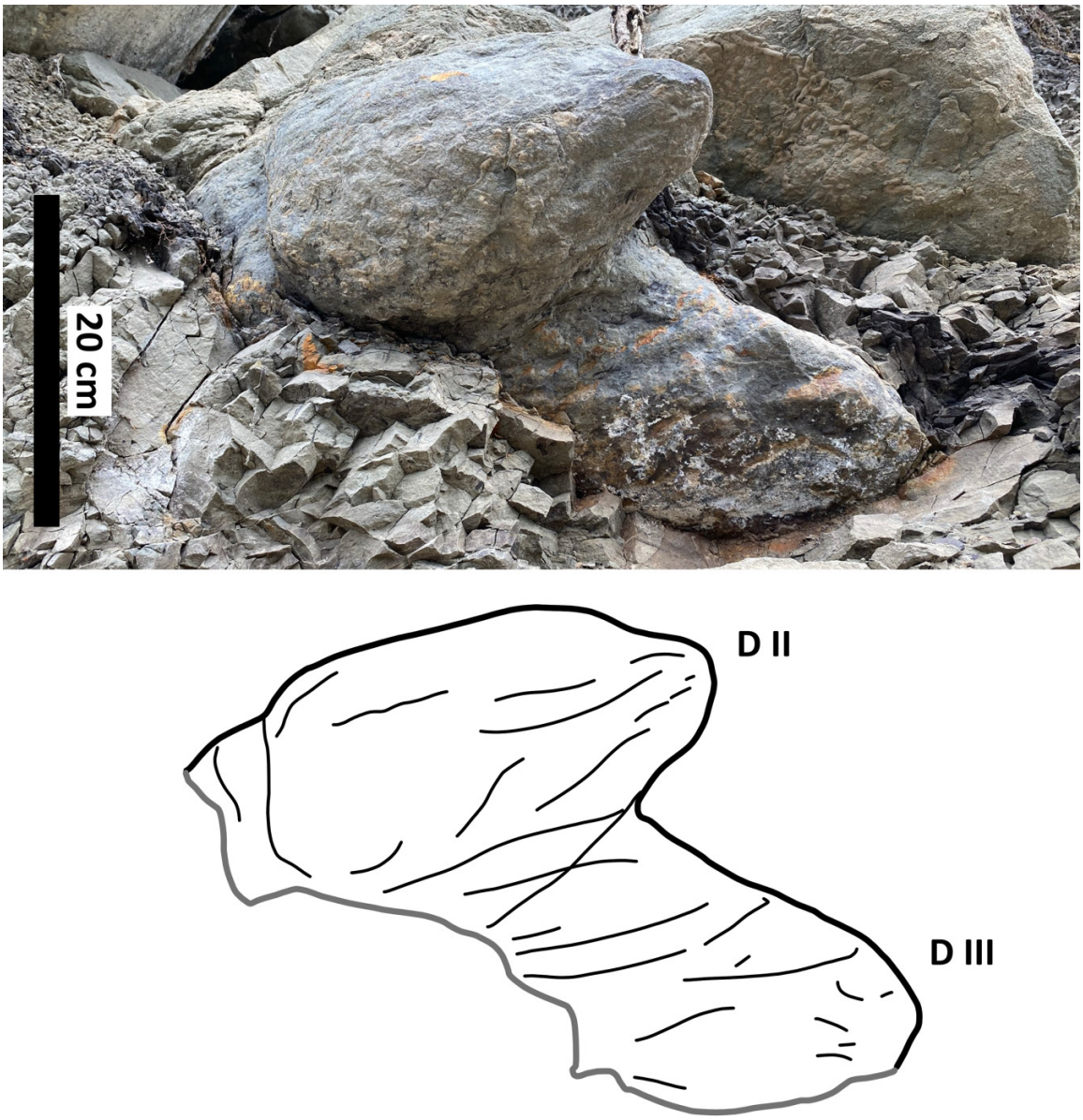

sandstone. Another ~60 cm of interbedded sandstone, ranging from very fine- (lower) to fine-grained (upper), overlies the rippled sandstone beds in a coarsening-upward trend. The lower 30 cm of this coarsening-upward package preserves symmetric ripples, many of which have mudstone drapes.

Above the coarsening upward packages, two fining upward packages are preserved (at ~31 to ~39.5 m). The base of both of these packages consist of fine-grained (upper) sandstone with current ripple-lamination. The top of the second fining-upward sandstone preserves symmetrical ripples before it transitions upwards into a set of interbedded siltstones and sandstones. Two sandstone (upper fine) packages (~45–51 and 56–59 m) possess nonerosional bases. Instead, both sandstones are deposited directly on top of siltstone (upper) where they infill densely spaced small (3 mm wide) inclined invertebrate burrows with no sign of disturbance. The intact nature of the burrows and the lack of an erosional base are interpreted as being evidence of the sandstone having been deposited in calm standing water.

The lacustrine deposits at ~29.5 m are interpreted as the highest local base-level represented in the section. Sediments immediately overlying the bonebed are interpreted to represent deposition lateral to a fluvial channel, with the overlying decimetre-scale interbedded sandstone and mudstone beds representing splays into water-saturated or subaqueous environments. Higher in the section, along Highway 40, the coarsening-upward siltstone to rooted muddy sandstone packages and a unit with interbedded sandstone and mudstone with symmetrical ripples indicate marginal lacustrine environments. The thickest lacustrine deposits from this sec-

Fig. 13. Sedimentary structures related to wet environments. (A) Sandstone structure interpreted as a pillow within underlying laminated siltstone 1.5 m above base of bonebed. Scale bar = 30 cm. (B) Stacked interbedded coarsening upward siltstone and sandstone beds. Dark grey siltstone is 19 m above base of bonebed. Scale = 20 cm. (C) Horizontal sandstone beds with large ripples at 25 m above bonebed base. Scale = 10 cm. (D) Horizontal beds with symmetrical ripples draped by overlying mudstone bed 29.5 m above bonebed base. Scale bar = 10 cm.

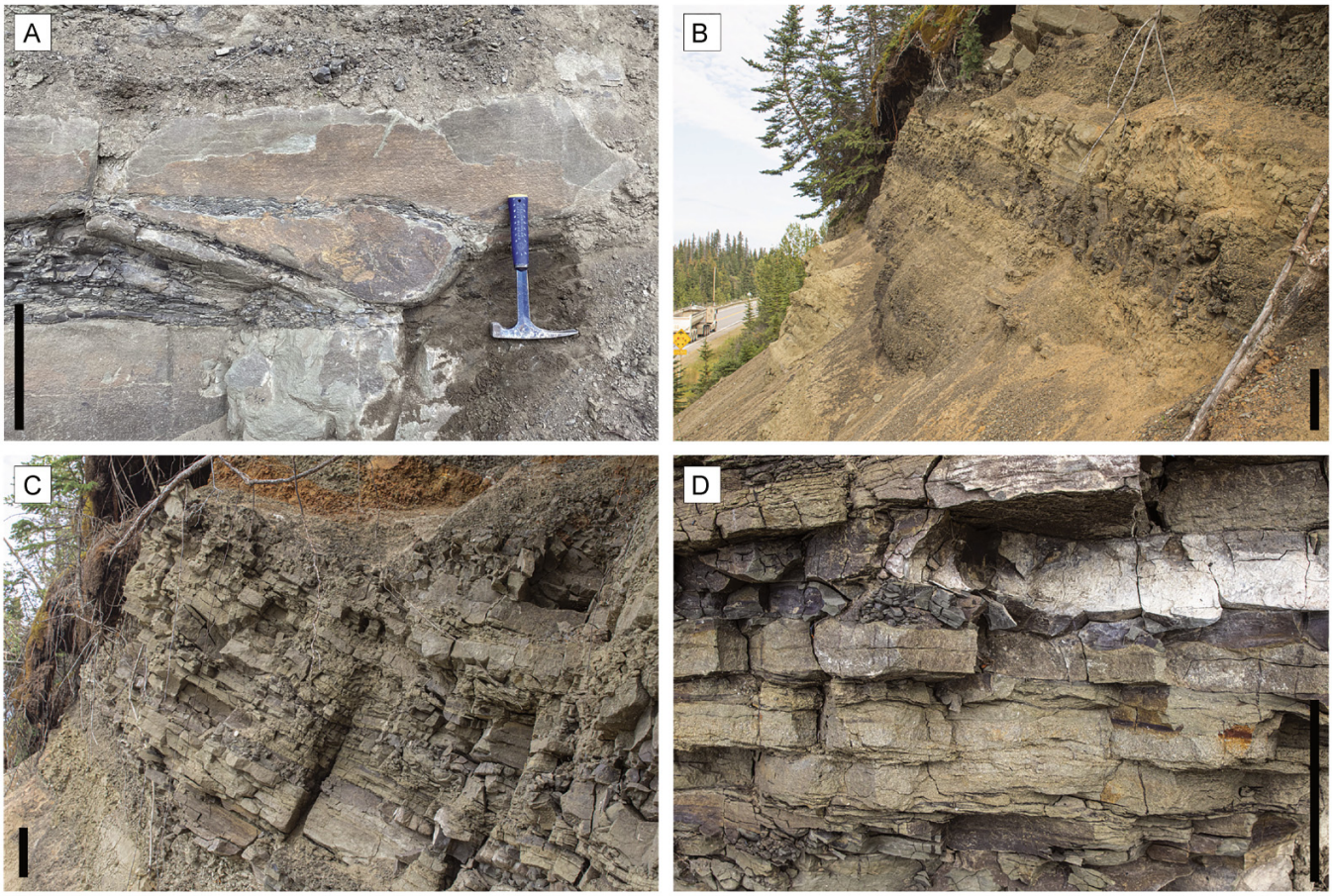

tion occur approximately 27 m above the bonebed, where a 40–50 cm thick interval of wave-ripple cross lamination and symmetrical ripple crests are present in the partly chert-cemented interlaminated sandstone and mudstone described above. Based on the sedimentary evidence in the succession, the depositional setting of the bonebed is interpreted as overbank deposition into a wet landscape in the early stages of an overall lake transgression.

The Hwy 40 section terminates at the Athabasca River ~20 m above the 60.60 m tephra, at which point the outcrop continues perpendicular along the Athabasca River (forming a single outcrop divided in two for this project, see Fig. 7). Where the Hwy 40 section meets the river section, several multistory sandstone packages are present and separated by ~10 m of vegetation covered siltstones. The base of the first large sand (~18.8 m above 60.60 m tephra) is interpreted as the contact between the middle and upper Brazeau Formation (Jerzykiewicz 1985*a*). Stratigraphically above these sandstone packages, the formation is almost completely covered by forest save for several small sections of exposure. Based on geological maps, and intact sandstones, the section is considered intact between 60.60 and 262.60 m tephras, with no identified tectonic faults that may impact the inferred sedimentation rate.

Geochronology

Zircon crystal morphology ranges from acicular to prismatic, showing magmatic oscillatory zoning, with some grains exhibiting sector zoning. Grains with obvious inherited cores were not analysed. The $^{206}Pb/^{238}U$ dates for the 28.15, 39.38, 39.68, 41.10, 51.78, 60.60, and 262.6 m tephras are remarkably coherent. However, the tephra at 23.75 m had significantly fewer zircons recovered (Fig. 6) and produced an approximate age of 70.71 ± 0.38 [0.61] Ma. The error-weighted means for zircon $^{206}Pb/^{238}U$ dates for the other tephras are as follows (errors in square brackets represent the 0.48% error from the 9435 reference; *n* indicates the number of zircons included in the error-weighted mean calculation out of the total number of zircons analyzed from the tephra sample): (1) 28.15 m = 70.10 ± 0.30|0.38 [0.52] Ma, *n* = 29/29; (2) 39.38 m = 69.60 ± 0.28 [0.42] Ma, *n* = 22/22; (3) 39.68 m = 69.66 ± 0.24 [0.42] Ma, *n* = 25/25; (4) 41.10 m = 70.28 ± 0.25 [0.44] Ma, *n* = 38/39; (5) 51.78 m = 69.92 ± 0.54 [0.77] Ma, *n* = 14/16;

Fig. 14. Monte Carlo sedimentation rate results. Median sedimentation rate results indicate approximately 447 m/Myr.

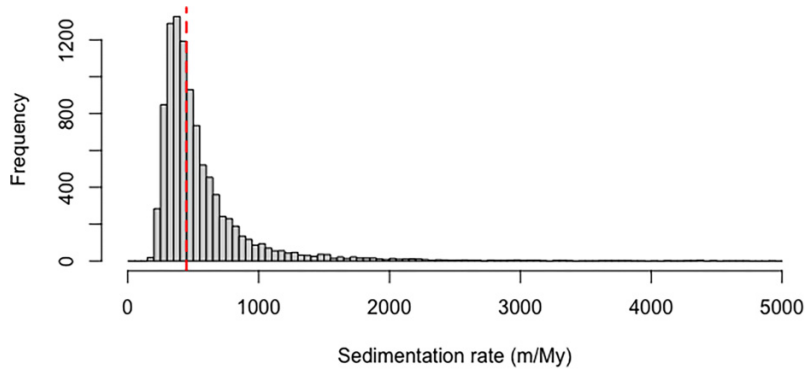

(6) 60.60 m = 69.72 ± 0.25|0.40 [0.52] Ma, n = 33/33; and (7) ~262.6 m = 69.60 ± 0.35 Ma, n = 17/19. The dates from these ashes indicate that the timing of pre-eruption zircon crystallization is statistically indistinguishable between the 7 beds with more than 10 zircons. The extrapolated bonebed age from the *Bchron* age model is 70.17 ± 0.42|0.38 Ma. The extrapolated age for the Sibley layer and the trackway horizon is 70.08 ± 0.26|0.31 Ma. These dates place the bonebed section within the middle Maastrichtian, equivalent to the upper Tolman Member of the HCF (Eberth and Kamo 2020) and unit 5 of the WF (Fanti and Catuneanu 2009). An extrapolated date of 69.73 ± 0.20|0.25 Ma for the contact between the middle and upper Brazeau Formation ~18 m above the 60.60 m tephra was derived using the age model. This date closely matches the calculated date of the contact between the Toleman and Carbon members of the HCF (69.6 ma; Eberth and Kamo 2020).

The median depositional rate across the section between the lowermost and uppermost dated tephra at 23.75 and 262.60 m was 447 m/Myr, with a 1σ range of 383–554 m/Myr and a 2σ range of 245–1752 m/Myr (Fig. 14).

Discussion

Timing and distribution of *Edmontosaurus*

The zircon $^{206}Pb/^{238}U$ dates from the eight sampled tephras in the ~262 m section at the Bennett Bonebed locality near Entrance, Alberta are the first known radiometric ages from the Brazeau Formation. The tephras yielded remarkably coherent distributions of zircon U–Pb dates with no modal groupings of dates from crystals erupted prior to the Cretaceous. For higher temporal precision, zircon U–Pb dating by single-grain thermal ionisation mass spectrometry (e.g., Davies et al. 2014) is needed to refine the extrapolated age for the Bennett Bonebed using the age-model developed from the tephra beds above the site. Bayesian statistics were employed to determine the most probable date of the trackway horizon, the Sibley layer, the Bennett Bonebed, and the contact between the middle and upper Brazeau Formation (~18.8 m above the measured section). Geological Survey of Canada samples (JO-83-1A and 1B) collected in 1983 from ~30 to 40 m above the bonebed at the same road-cut section described here yielded two palynomorphs, *Aquilapollenites* (including *Aquilapollenites augustus*, *Aquilapollenites drumhellerensis*, *Aquilapollenites funkhouseri*, and *Aquilapollenites leucocephalus*) and *Kurtzipites andersonii*, that were identified by Sweet (1987) as palynostratigraphic markers for the early to middle Maastrichtian age.

Edmontosaurus is a well known and widely distributed genus from Wyoming north to Alaska, and it spans approximately 6 million years, from 72.5 to 66 Ma (Fig. 15) (Lambe 1917; Campione and Evans 2011; Evans et al. 2015; Mori et al. 2016; Xing et al. 2017). *Edmontosaurus regalis* is common in Alberta and is most abundant in the HCF (Lambe 1917; Evans et al. 2015; Xing et al. 2017). Within the HCF, *Edmontosaurus regalis* is known primarily from the Horsethief Member with some tentative remains from the Upper Drumheller Member, which represents a certain temporal span of 72.2–71.5 Ma, and potentially 73.1–71.5 Ma (Eberth et al. 2013; Evans et al. 2015; Eberth and Kamo 2020). A partial *Edmontosaurus regalis* specimen with preserved skin impressions (UALVP 53722) was recovered from the WF, 2 m below a tephra deposit dated using $^{40}Ar/^{39}Ar$ to 72.58 ± 0.09 Ma (Bell et al. 2014). *Edmontosaurus regalis* thus has an age range of at least 0.92 million years, from ~72.6 to 71.5 Ma, using the ages from both the HCF and the WF. The Liscomb bonebed in the Prince Creek Formation of northern Alaska, dated to 69.2 ± 0.5 Myr (Mori et al. 2016), has produced specimens of *Edmontosaurus* sp.; however, the Alaskan taxon requires further adult material to determine the species represented (Takasaki et al. 2020). *Edmontosaurus annectens* has been reported from the upper Maastrichtian of Saskatchewan, Canada, and Colorado, Montana, North and South Dakota, and Wyoming in the U.S.A, spanning approximately 1.2 Myr, from 65.5 to 66.7 Ma (Campione and Evans 2011). Unfortunately, the two postorbitals reported herein do not provide enough information to identify the taxon within the Bennett Bonebed to species level with high confidence. Although the species cannot be confidently identified, based on the enlarged postorbital fossa, further work in the bonebed may conclude that the assemblage comprises *Edmontosaurus regalis*. However, due to the age of the oldest known *Edmontosaurus regalis* (~72.5 Ma), it would be unlikely that a single species would span ~2.5 Myr. For this reason, the Bennett Bonebed assemblage may represent a new species of *Edmontosaurus*, al-

Fig. 15. Temporal distribution and regions from which *Edmontosaurus* has been recovered. Circles indicate costal plains, triangles are coastal wet environments, stars indicate upland environments. Brazeau *Edmontosaurus* sp. zone appears gradational to reflect age uncertainty.

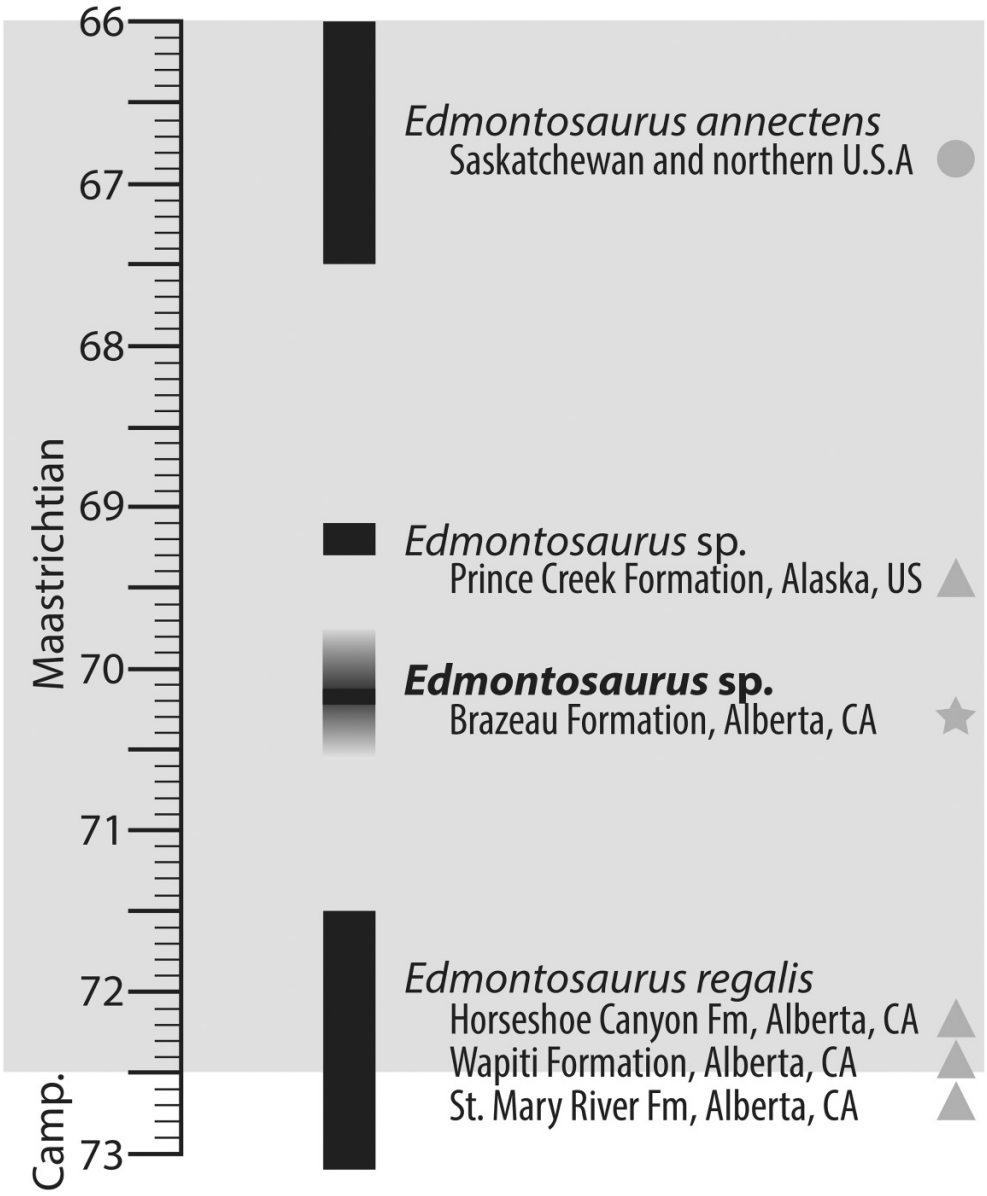

though further diagnostic elements, such as the frontal, need to be recovered. For the same reason, the Prince Creek Formation *Edmontosaurus* sp. is not being referred to as either *Edmontosaurus regalis* or *Edmontosaurus annectens*, despite Sharpe et al. (2023) referring it to *Edmontosaurus regalis* due to the similarities between cranial elements of similarly sized juvenile remains. Rapid lambeosaurine faunal turnover rates of the Dinosaur Park Formation (i.e., *Corythosaurus casuarius* and *Corythosaurus intermedius* ~750 kyr; *Lambeosaurus clavinitalis*, *Lambeosaurus lambei*, and *Lambeosaurus magnicrisatus* ~1 Ma; Mallon 2019; Ramezani et al. 2022), moderate lambeosaurine turnover rates in the HCF *Hypacrosaurus altispinus* ~1.9 Ma; (Eberth and Kamo 2020) and moderate saurolophine turnover rates in the Dinosaur Park Formation (*Prosaurolophus maximus* ~1.75 Ma; Drysdale et al. 2018), and the HCF all suggest that is unlikely that a single species would have persisted for ~4 Myr.

The palaeoenvironments represented by the sediments associated with the bonebed are interpreted as a water-saturated to submerged environment, becoming distinctly lacustrine approximately 27 m above the bonebed (Figs. 8 and 13). Evidence for this interpretation includes loaded and swirled sediments, coarsening-upward packages, planar interbedded sandstone and siltstone, flat-lying undisturbed volcaniclastic ashes with sharp lower and upper surfaces, laminated mudstone, and symmetrical ripple bedforms and lamination. Rootlets present in thinly bedded and laminated lacustrine sediments with symmetrical ripples are interpreted as roots of shallow water flora or from brief periods of exposure in a lake-marginal setting. The Bennett Bonebed is in-

terpreted to have been deposited during a flood event into a wet area adjacent to a channel, perhaps in the upper reaches of a lacustrine delta where standing water accumulated in lows between distributary channels. This is supported by a sandstone bed with a loaded base that overlies shale found directly above the bonebed layer.

The footprints described here are the first hadrosaur prints reported for the Brazeau Formation, with an extrapolated date of ~70.08 ± 0.26|0.31 Ma. The skeletal remains from the bonebed horizon (meter 2.90 in the measured section) are the first evidence of *Edmontosaurus* sp. from the Brazeau Formation, expanding the geographic and temporal range of the genus in Alberta. Although other known specimens of *Edmontosaurus* from Alberta tend to be associated with swampy/coaly environments on the coastal plain or alluvial plain adjacent to the Western Interior Seaway (Russell and Chamney 1967; Fanti and Catuneanu 2009; Eberth and Braman 2012; Bell and Campione 2014; Eberth et al. 2014; Eberth and Kamo 2020), no coal beds have been observed in the area around the Bennett Bonebed. Instead, lacustrine and lake marginal environments were present, and the bonebed site may represent a proximal lake delta-plain setting. Roots in coarsening upwards homogenous siltstones to very fine-grained sandstones above the bonebed also indicate a well vegetated setting; the palaeoenvironment is interpreted to be marginal lacustrine wetlands. Eberth et al. (2013) discussed the palaeoecology of *Edmontosaurus regalis* and suggested that the taxon preferred saturated deltaic wetlands, suffering extirpation from the lower HCF environments when the landscape became drier and better drained. Although Eberth et al. (2013) did not propose where *Edmontosaurus regalis* might have moved to, the species could have migrated southeastward with the Western Interior Seaway coastal plain during regression expressed in the HCF. It is also possible that *Edmontosaurus regalis* migrated westward toward the wet landscape represented in the Brazeau Formation, and later, north to the coastal plains of Alaska. The lacustrine deposits of the Brazeau Formation exposed around the Bennett Bonebed support the hypothesis that *Edmontosaurus* preferred a wet environment, although the habitat need not have been coastal coal swamps.

The inferred ~70.17 Ma age for the Bennett Bonebed makes UALVP 59617 and UALVP 60423 the only positively identified *Edmontosaurus* sp. (Saurolophinae) specimens currently known from the middle of the Maastrichtian outside of Alaska. The Bennett Bonebed is temporally equivalent to the top of the upper Tolman Member of the HCF (Eberth et al. 2013), in which there are two other known hadrosaur taxa during this interval, *H. altispinus* (Lambeosaurinae) and *Saurolophus osborni* (Saurolophinae). The age and associated lake-margin palaeoenvironments of the Bennett Bonebed and hadrosaur footprint layer have interesting implications. First, *Edmontosaurus* inhabited a region a significant distance from the Western Interior Seaway coastal plain swamps, as the shoreline at the time of the upper Tolman Member was at least >325 km southeastward (at Dorothy, Alberta) of the Bennett Bonebed site (Eberth et al. 2013) and potentially up to a distance of ~750 km to time-equivalent beds in the Eastend Formation of southern Saskatchewan (Broughan 1984). Although the animals in the Bennett Bonebed lived in an environment with potentially large bodies of water nearby, the site is in an unexpected palaeogeographical area for *Edmontosaurus*, further west than previously known. This indicates that the taxon may be more widespread across the middle Maastrichtian landscape than previously anticipated, and/or that *Edmontosaurus* migrated westward as well as eastward when the HCF environments became drier (cf. Eberth et al. 2013). Future work in regions discovered to preserve lacustrine deposits should consider the possibility that typically "coastal" taxa may be present. Second, the discovery of *Edmontosaurus* ~1.3 Ma after its extirpation from the HCF environments suggests that either *Edmontosaurus regalis* persisted for more than 1 million years longer than previously known, with a total time span of nearly 2.5 Myr, or that the specimens in the Bennett Bonebed represent a previously unknown species of the genus.

Further work in the Bennett Bonebed will hopefully provide additional information as to the taxonomic assignment of the species, which may provide an opportunity to infer allopatric speciation in the fossil record of hadrosaurs. If the climate change event at ~71.5 Ma that resulted in the extirpation of *Edmontosaurus* in the HCF (cf. Eberth et al. 2013) drove the genus south along the coast into the USA or to the north into Alaska, then a physical environmental barrier in the form of a well drained, cool, dry landscape would have separated outside populations from that in the Brazeau Formation. Speciation may have occurred if this separation persisted for the ~1.3 Myr observed in the palaeontological record.

Basin-scale setting and sedimentation rates of Brazeau Formation at Entrance, Alberta

The Rundle orogenic pulse occurred during the late Campanian (Pană and van der Pluijm 2014). Several thrust faults west of the Bennett Bonebed have been dated using authigenic illite (Pană and van der Pluijm 2014); these dates contribute to a better understanding of the subsequent palaeogeography of the central foothills of Alberta during the early Maastrichtian by providing a predictable location for the palaeo-mountain front. The dated fault that is closest in age and proximity to the Bennett Bonebed is known as the Rocky Pass Thrust fault (74.8 Ma; Pană and van der Pluijm 2014) (Fig. 5), which is presently exposed 37 km to the west of the site. Based on the available geological cross-sections from the Entrance area, the palaeogeographical distance from the bonebed to the Rocky Pass Thrust is estimated to have been 55 km during deposition of the bonebed (Alberta Geological Survey Map 560; Pana and Elgr 2013). This places the Bennett Bonebed specimens close to the palaeo-Rocky Mountains and indicates that the animals preserved here may have lived in a more topographically diverse environment than on the coastal plain represented by the HCF in eastern Alberta. Sedimentation rates reported by Eberth and Kamo (2020) for the upper Tolman Member (~16 m/Myr) were interpreted to represent an increase in tectonic uplift to the west, and a subsequent decrease in the rate of subsidence in the upper HCF near Drumheller.

We calculated a median total section sedimentation rate of 447 m/Myr. However, this sedimentation rate at the study site should be considered as a rough estimate only because the statistically indistinguishable zircon dates yield a wide range of accumulation rates that are difficult to objectively constrain (1σ range of 383–554 m/Myr; 2σ range of 245–1752 m/Myr; Fig. 14). Related challenges include the relatively high uncertainty of LA-ICP-MS analyses (compared to, e.g., single-grain chemical abrasion isotope-dilution thermal ionisation mass spectrometry) and the possible incorporation of xenocrystic and antecrystic zircon.

Nevertheless, the 447 m/Myr median calculated sedimentation rate is substantially higher than for other Campanian and Maastrichtian formations in Alberta: (1) Dinosaur Park Formation (~36.6 m/Myr) (Ramezani et al. 2022); (2) HCF (~81 m/Myr for the lower two-thirds and ~16 m/Myr for the upper third) (Eberth and Kamo 2020); (3) WF (~60 m/Myr) (Fanti and Catuneanu 2009); and (4) the Scollard Formation (calculation based on data in Eberth and Kamo (2020) of ~43 m/Myr). It also outpaces sedimentation rates of other Laramidian formations, such as the Campanian Judith River Formation (~44.2 m/Myr) (Ramezani et al. 2022) and Campanian Two Medicine Formation (~62.1 m/Myr) (Ramezani et al. 2022), both exposed in Montana.

The range of plausible sedimentation rates for the Brazeau Formation at Entrance, Alberta is within the same order of magnitude as the Campanian Kaiparowits Formation of Utah (372 m/Myr) (Ramezani et al. 2022). The Kaiparowits Formation was also deposited within a foreland basin, with sediment partly supplied from a surrounding active thrust fault system (Lawton and Bradford 2011; Beveridge et al. 2020; Ramezani et al. 2022). The subsidence of the Kaiparowits basin within ~25–30 km of the Sevier Orogenic Belt during active tectonism resulted in a significant amount of sediment accumulating relatively quickly (620 m over ~2 Myr) (Ramezani et al. 2022). Similarly, the Eocene Green River Formation (~54.5–42 Myr) was formed in a tectonically active region, with thrusting and reactivated basement faults producing a series of small lake basins in a "broken foreland" (e.g., Smith et al. 2008). The Bridger Basin, a subbasin in the Greater Green River Basin of Wyoming, was surrounded by several uplifts: the Sevier fold and thrust belt to the west, the Wind River Uplift to the north, the Rock Springs Uplift to the east, and the Uinta Uplift to the south (Smith et al. 2008). In areas adjacent to the uplifts, sedimentation rates were typically high. The Wilkins Peak Member adjacent to the Uinta Uplift, for example, was ~360 m/Myr within ~30 km of the uplift in predominantly lake-marginal environments (Smith et al. 2008, 2015). The Bridger Member of the Green River Formation, which represents the final fill of the Bridger Basin, records very rapid sedimentation rates of >1000 m/Ma at the base, when volcaniclastics were transported into the basin from the north (Smith et al. 2008; Aswasereelert et al. 2013). This high sedimentation rate indicates that within a basin of a tectonically active region, clastic deposition can increase quickly, and the high rate inferred for the outcrop in the study area is not surprising.

The depositional location of the Bennett Bonebed being so close to the Rocky Pass Thrust in palaeo-Rocky Mountains (~55 km SW) indicates that it was close to or within the foreland basin depocenter during the Maastrichtian. The estimated sedimentation rate of ~380–550 m/Myr for the study area is plausible if the foreland basin was subsiding in response to the front range thrust-faulting event dated by Pană and van der Pluijm (2014). Additionally, high rates of sedimentation likely originated from the palaeo-Athabasca River as a possible broad alluvial fan as it exited the paleo-Rocky Mountains as the river would have been present close to the Bennett Bonebed.

Douglass et al. (2009) proposed a criteria-based methodology to determine the method of transverse drainage development. Because the source area for the palaeo-Athabasca River is older than the front ranges through which it cuts, two possible mechanisms of valley formation are possible. First, antecedence occurs when large rivers incise through a bedrock high (i.e., mountain range(s)) as the river maintains a relatively stable elevation and the bedrock is tectonically lifted around it, resulting in a valley. The second, superimposition, occurs when the bedrock high is already in place but buried by different sediments with a river flowing over it. Subsequently, the river erodes down through the overlaying sediments and the bedrock high to form a valley (Douglass et al. 2009). In the case of the Rocky Mountain front and the palaeo-Athabasca River, superimposition as a mechanism would be nearly impossible, as it would require the entire Rocky Mountain belt to be completely buried in secondary sediments with the headwaters originating from an unpreserved high somewhere near the modern source. Because the front ranges formed ~86 Myr after the origin of the Athabasca River headwaters was uplifted (Pană and van der Pluijm 2014), the river would have been cutting through the mountains as they grew, as modelled in the antecedence mechanism of transverse drainages. It is therefore likely that during the deposition of the Bennett Bonebed, the palaeo-Athabasca River would have exited the palaeo-Rocky Mountains southwest of the study area near the Rocky Pass Thrust (Fig. 5). Draining at least 4000–5000 km^2 of mountainous terrain (based on hydrometric data from the Government of Canada) out into the immediate basin along the palaeo-mountain front, the palaeo-Athabasca would have provided a significant source of sediment, especially during periods of thrusting, directly into the developing foreland basin in the region around the Bennett Bonebed.

Although the recorded Bennett Bonebed sedimentary section only records the equivalent of the upper Tolman Member, the high rate of sedimentation (~380–550 m/Myr) and the presence of lakes in the Brazeau Formation in our study area provide evidence that subsidence rates in the proximal foredeep were high, supporting the hypothesis proposed by Eberth and Kamo (2020) that there was an increase in tectonic uplift sometime after 70.6 Ma. Additionally, the nine tephras (eight dated herein and one undated) distributed across 238.85 m (lowest to highest tephras) of the stratigraphic section in the road-cut near the Bennett Bonebed suggest that there was significant volcanic activity in the region west of the site during the middle Maastrichtian. However, this volcanism is not as readily recorded or was not preserved further east in the basin, resulting in few datable tephras in

the Tolman Member of the Horseshoe Canyon Fm. in Alberta and the Judith River Fm. in Montana (Eberth and Kamo 2020; Fanti et al. 2022; Ramezani et al. 2022; Rogers et al. 2023).

Brazeau Formation stratigraphy and correlation of the Entrance road-cut section

The middle and upper Brazeau Formation contact (Cyclothems III-b and IV-a) is exposed approximately 18.8 m (calculated by GPS-calibrated orthographic image) above the 60.60 m tephra at the eastern end of the Hwy 40 bridge crossing the Athabasca River. In the ~60 m measured section at the road-cut, there is an abrupt change from the very fine-grained (mudstones, siltstones, and very fine-grained sandstones) lake-marginal and lacustrine deposits to multiple stacked, multistory thick sandstones at ~79.4 m above the base of the section (Fig. 7); this is interpreted as the contact between the middle and upper Brazeau Formation. The lower half of the upper Brazeau (Cyclothem IV-a) is at least 75 m thick (measured from the orthographic images produced from drone photography), and the upper half at this locality is currently an unknown thickness. Using the position of ~18.8 m above the 60.60 m tephra for the middle/upper Brazeau contact obtained from the orthographic image, an extrapolated date using the age-model for the base of the upper Brazeau Formation was calculated to ~69.73 + 0.20, −0.25 Ma. This median date aligns closely with the bottom of Carbon Member of the HCF, which is reported to be ~69.6 Ma (Eberth and Kamo 2020). Eberth and Kamo (2020) report that a change in climate from the cool-dry climate of the Tolman Member gradually reversed back to a warm-wet climate in the Carbon Member above.

Conclusions

The identification and description of *Edmontosaurus* sp. postorbitals from the Bennett Bonebed represent the first identified taxon and the first described vertebrate remains from the Brazeau Formation. The postorbitals are identified as *Edmontosaurus* sp. by an enlarged postorbital fossa, a feature that is presently known in this genus. Based on the size, the more complete UALVP 59617 is from a juvenile individual, and UALVP 60423 is from a sub-adult.

Radiometric dates obtained from eight tephra beds provide a probable date of ~70.08 Ma for the Sibley layer and associated hadrosaur trackways, and a date of ~70.17 Ma for the bonebed, placing it in the middle Maastrichtian. Sweet's (1987) identification of *Aquilapollenites* and *K. andersonii* palynomorphs in sediments ~30–40 m stratigraphically higher than the bonebeds is consistent with placement within the middle Maastrichtian, though there is substantial diachroneity in the occurrence of *Aquilapollenites* in North America (e.g., Braman 2001; Buryak et al. 2024). Together with radiometric and palynological dating, these new specimens from the Bennett Bonebed provide sufficient evidence that the genus *Edmontosaurus* persisted in Alberta well into the Maastrichtian and was coeval, but not sympatric with *Hypacrosaurus* and *Saurolophus* in the upper Tolman Member of the HCF. Continued exploration of the Brazeau Formation and Bennett Bonebed are vital in further understanding the biogeographic distribution of *Edmontosaurus* in the early Maastrichtian and may provide evidence of the origin of *Edmontosaurus annectens*.

The stratigraphic contact of the middle and upper Brazeau Formation from the measured section is calculated using the age-model presented here to ~69.73 Ma, which corresponds well to the approximate date for the base of the Carbon Member in the HCF. This may indicate that the climate shift event that is interpreted to have occurred in the Carbon Member could be the same event that influenced the formation of the thick sandstone units present in the upper Brazeau Formation at Entrance, Alberta. Additionally, the high rate of sedimentation in the Brazeau Formation at the study site, during a time-equivalent period of low sedimentation rate in the upper HCF, supports the hypothesis of Eberth and Kamo (2020) that there was an increase in tectonism in the paleo-Rocky Mountains at this time.

Acknowledgements

We thank Dana Bennett for her kindness and support in excavating the bonebed. Without her assistance, this research would not have been possible, as well as the Olea family for their continued permission to the dig site. Thank you to Jailin Bertolin for accommodations throughout the bonebed excavation. David Evans (ROM), Jordan Mallon (CMN), Scott Rufolo (CMN), and Corwin Sullivan (UA) provided images of specimens for line drawings, and Ryan McKellar (RSM) provided access to specimens. Thank you to Mike Ranger for providing the stratigraphic logging software Applecore. Kate Pearson gracefully provided copies of the historical Barnum Brown letters to R.C. Sibley. We would also like to thank Luis Buatois and M. Gabriela Mángano for feedback that improved the manuscript. We thank Zane McNaught, Stewart Barg, and Victoria Mauer for field assistance during the measuring of the stratigraphic section, and Lavonne Schill, Khoi Nguyen, and Caelin Libke for assistance with excavation of the bonebed test pit. The Dinosaur Research Institute funded the 2018 Mountainous Alberta Dinosaur Project (MADP), during bonebed excavation; van der Reest also acknowledges a Dean's scholarship from the University of Saskatchewan. Currie, Reyes, and Scott acknowledge support from the NSERC Discovery Grant program, which funded the fieldwork and zircon geochronology. Mount Royal University provided field-mapping equipment. Drone imagery was processed using software sponsored by Agisoft.

Article information

History dates

Received: 1 January 2023
Accepted: 18 April 2025
Accepted manuscript online: 16 September 2025
Version of record online: 30 October 2025

Data availability

As the quarry is located on private property, precise locality data are retained at the University of Alberta Laboratory for Vertebrate Palaeontology, and can be obtained for research purposes upon permission by landowner/first author.

Author information

Author ORCIDs

Aaron J. van der Reest https://orcid.org/0000-0002-6000-4623
Alberto V. Reyes https://orcid.org/0000-0002-7838-4214
Philip J. Currie https://orcid.org/0000-0001-6857-3161

Author notes

Alberto V. Reyes served as Associate Editor at the time of manuscript review and acceptance; peer review and editorial decisions regarding this manuscript were handled by another editorial board member.

Author contributions

Conceptualization: AJvdR
Data curation: AJvdR, SAD
Formal analysis: AJvdR, SAD
Funding acquisition: AJvdR, AVR, PJC, JJS
Investigation: AJvdR, SAD, JJS
Methodology: AJvdR, AVR
Project administration: PJC
Software: AJvdR
Supervision: PJC, JJS
Writing – original draft: AJvdR, SAD
Writing – review & editing: AJvdR, AVR, PJC, JJS

Competing interests

There are no competing interests with this research, financial or otherwise.

Supplementary material

Supplementary data are available with the article at https://doi.org/10.1139/cjes-2023-0001.

References

Aswasereelert, W., Meyers, S.R., Carroll, A.R., Peters, S.E., Smith, M.E., and Feigl, K.L. 2013. Basin-scale cyclostratigraphy of the Green River Formation, Wyoming. Geological Society of America Bulletin, **125**: 216–228. doi:10.1130/B30541.1.

Bell, P.R., and Campione, N.E. 2014. Taphonomy of the Danek Bonebed: a monodominant *Edmontosaurus* (Hadrosauridae) bonebed from the Horseshoe Canyon Formation, Alberta. Canadian Journal of Earth Sciences, **51**: 992–1006. doi:10.1139/cjes-2014-0062.

Bell, P.R., Fanti, F., Currie, P.J., and Arbour, V.M. 2014. A mummified duck-billed dinosaur with a soft-tissue cock's comb. Current Biology, **24**: 70–75. doi:10.1016/j.cub.2013.11.008. PMID: 24332547.

Beveridge, T.L., Roberts, E.M., and Titus, A.L. 2020. Volcaniclastic member of the richly fossiliferous Kaiparowits Formation reveals new insights for regional correlation and tectonics in southern Utah during the latest Campanian. Cretaceous Research, **114**: 1–22. doi:10.1016/j.cretres.2020.104527.

Braman, D.R. 2001. Terrestrial palynomorphs of the upper santonian-? Lowest Campanian Milk River Formation, southern Alberta, Canada. Palynology, **25**: 57–107. doi:10.1080/01916122.2001.9989556.

Broughan, F.M. 1984. Paleoenvironment of the Eastend, Whitemud (Maastrichtian), and Ravenscrag (Paleocene) formations in eastern Cypress Hills, Saskatchewan. MSc Thesis, University of Saskatchewan, p. 178.

Buryak, S.D., Reyes, A.V., West, C.K., Jensen, B.J.L., DuFrane, S.A., Davies, J.H.F.L., et al. 2024. Tephra zircon U-Pb geochronology of kimberlite maar sedimentary fills in subarctic Canada: implications for Eocene paleoclimate and Late Cretaceous paleogeography. Geological Society of America Bulletin, **136**: 3921–3938. doi:10.1130/B37276.1.

Campbell, J.A., Ryan, M.J., and Anderson, J.S. 2020. A taphonomic analysis of a multitaxic bonebed from the St. Mary River Formation (uppermost Campanian to lowermost Maastrichtian) of Alberta, dominated by cf. *Edmontosaurus regalis* (Ornithischia: Hadrosauridae), with significant remains of *Pachyrhinosaurus*. Canadian Journal of Earth Sciences, **57**: 617–629. doi:10.1139/cjes-2019-0089.

Campione, N.E., and Evans, D.C. 2011. Cranial growth and variation in *Edmontosaurs* (Dinosauria: Hadrosauridae): implications for latest Cretaceous megaherbivore diversity in North America. PLoS ONE, **6**: e25186. doi:10.1371/journal.pone.0025186.

Davies, J.H.F.L., Wotzlaw, J.-F., Wolfe, A.P., Heaman, L.M., and Arbour, V. 2014. Assessing the age of the Late Cretaceous Danek Bonebed with U–Pb geochronology. Canadian Journal of Earth Sciences, **51**: 982–986. doi:10.1139/cjes-2014-0136.

Dawson, M., and Kalkreuth, W. 1994. Coal rank and coalbed methane potential of Cretaceous/tertiary coals in the Canadian Rocky Mountain foothills and adjacent foreland: 1. Hinton and Grande Cache areas, Alberta. Bulletin of Canadian Petroleum Geology, **42**: 544–561.

Douglas, R.J.W. 1958. Chungo Creek Map-area Alberta (83C/9). Geological Survey of Canada Paper 58-3.

Douglas, R.J.W., and MacKay, B.R. 1953. Map 6-1958, Chungo Creek, West of Fifth Meridian, Alberta: to accompany paper 58-3. Department of Mines and Technical Surveys, Geological Survey of Canada.

Douglass, J., Meek, N., Dorn, R.I., and Schmeeckle, M.W. 2009. A criteria-based methodology for determining the mechanism of transverse drainage development, with application to the Southwestern United States. Geological Society of America Bulletin, **121**: 586–598. doi:10.1130/B26131.1.

Drysdale, E.T., Therrien, F., Zelenitsky, D.K., Weishampel, D.B., and Evans, D.C. 2018. Description of juvenile specimens of *Prosaurolophus maximus* (Hadrosauridae: Saurolophinae) from the Upper Cretaceous Bearpaw Formation of southern Alberta, Canada, reveals ontogenetic changes in crest morphology. Journal of Vertebrate Paleontology, **38**: e1547310. doi:10.1080/02724634.2018.1547310.

Eberth, D.A. 2015. Origins of dinosaur bonebeds in the Cretaceous of Alberta, Canada. Canadian Journal of Earth Sciences, **52**: 655–681. doi:10.1139/cjes-2014-0200.

Eberth, D.A., and Braman, D.R. 2012. A revised stratigraphy and depositional history for the Horseshoe Canyon Formation (Upper Cretaceous), southern Alberta plains. Canadian Journal of Earth Sciences, **49**: 1053–1086. doi:10.1139/e2012-035.

Eberth, D.A., and Kamo, S.L. 2020. High-precision U–Pb CA–ID–TIMS dating and chronostratigraphy of the dinosaur-rich Horseshoe Canyon Formation (Upper Cretaceous, Campanian–Maastrichtian), Red Deer River valley, Alberta, Canada. Canadian Journal of Earth Sciences, **57**: 1220–1237. doi:10.1139/cjes-2019-0019.

Eberth, D.A., Bell, P.R., and Arbour, V. 2014. Stratigraphy of the Danek Bonebed (Upper Cretaceous Horseshoe Canyon Formation, central Alberta) and correlations with strata in the Drumheller and Grande Prairie regions[1]. Canadian Journal of Earth Sciences, **51**: 975–981. doi:10.1139/cjes-2014-0069.

Eberth, D.A., Evans, D.C., Brinkman, D.B., Therrien, F., Tanke, D.H., and Russell, L.S. 2013. Dinosaur biostratigraphy of the Edmonton Group (Upper Cretaceous), Alberta, Canada: evidence for climate influence. Canadian Journal of Earth Sciences, **50**: 701–726. doi:10.1139/cjes-2012-0185.

Evans, D.C., Eberth, D.A., and Ryan, M.J. 2015. Hadrosaurid (*Edmontosaurus*) bonebeds from the Horseshoe Canyon Formation (Horsethief Member) at Drumheller, Alberta, Canada: geology, preliminary taphonomy, and significance. Canadian Journal of Earth Sciences, **52**: 642–654. doi:10.1139/cjes-2014-0184.

Fanti, F., and Catuneanu, O. 2009. Stratigraphy of the Upper Cretaceous Wapiti Formation, west-central Alberta, Canada. Canadian Journal of Earth Sciences, **46**: 263–286. doi:10.1139/E09-020.

Fanti, F., Bell, P.R., and Sissons, R.L. 2013. A diverse, high-latitude ichnofauna from the Late Cretaceous Wapiti Formation, Alberta, Canada. Cretaceous Research, **41**: 256–269. doi:10.1016/j.cretres.2012.12.010.

Fanti, F., Bell, P.R., Vavrek, M., Larson, D., Koppelhus, E., Sissons, R.L., et al. 2022. Filling the Bearpaw gap: evidence for palaeoenvironment-driven taxon distribution in a diverse, non-marine ecosystem from the late Campanian of west-Central Alberta, Canada. Palaeogeography, Palaeoclimatology, Palaeoecology, **592**: 110923. doi:10.1016/j.palaeo.2022.110923.

Gilbert, M.M., Buatois, L.A., and Renaut, R.W. 2020. Stratigraphy and depositional environments of the Belly River Group (Campanian) in southwestern Saskatchewan, Canada. Bulletin of Canadian Petroleum Geology, **68**: 31–63. doi:10.35767/gscpgbull.68.2.31.

Gunther, P.R., and Hills, L.V. 1972. Megaspores and other palynomorphs of the Brazeau Formation (Upper Cretaceous), Nordegg Area, Alberta. Geoscience and Man, **4**: 29–48. doi:10.1080/00721395.1972.9989717.

Hamblin, A.P., and Abrahamson, B.W. 1996. Stratigraphic architecture of "Basal Belly River" cycles, Foremost Formation, Belly River Group, subsurface of southern Alberta and southwestern Saskatchewan. Bulletin of Canadian Petroleum Geology, **44**: 654–673.

Haslett, J., and Parnell, A.C. 2008. A simple monotone process with application to radiocarbon-dated depth chronologies. Journal of the Royal Statistical Society: Series C, **57**: 399–418. doi:10.1111/j.1467-9876.2008.00623.x.

Jackson, S.E., Pearson, N.J., Griffin, W.L., and Belousova, E.A. 2004. The application of laser ablation-inductively coupled plasma-mass spectrometry to in situ U-Pb zircon geochronology. Chemical Geology, **211**: 47–69. doi:10.1016/j.chemgeo.2004.06.017.

Jerzykiewicz, T. 1985a. Stratigraphy of the Saunders Group in the central Alberta Foothills–a progress report. *In* Current research, part B, paper 85-1. Geological Survey of Canada. pp. 247–258.

Jerzykiewicz, T. 1985b. Techtonically deformed pebbles in the Brazeau and Paskapoo Formation, central Alberta foothills, Canada. Sedimentary Geology, **42**: 159–180. doi:10.1016/0037-0738(85)90043-0.

Jerzykiewicz, T. 1997. Stratigraphic framework of the Uppermost Cretaceous to Paleocene strata of the Alberta basin. Geological Survey of Canada Bulletin, **510**: 1–121.

Jerzykiewicz, T., and McLean, J.R. 1980. Lithostratigraphical and sedimentological framework of coal-bearing Upper Cretaceous and lower tertiary strata, Coal Valley area, central Alberta foothills. Geological Survey of Canada Paper, **79–12**: 1–47.

Jerzykiewicz, T., and Sweet, A.R. 1988. Sedimentological and palynological evidence of regional climatic changes in the Campanian to Paleocene sediments of the Rocky Mountain foothills, Canada. Sedimentary Geology **59**: 29–76.

Klepeis, K.A., Crawford, M.L., and Gehrels, G. 1998. Structural history of the crustal-scale Coast shear zone north of Portland Canal, southeast Alaska and British Columbia. Journal of Structural Geology, **20**: 883–904. doi:10.1016/S0191-8141(98)00020-0.

Lambe, L.M. 1917. A new genus and species of crestless hadrosaur from the Edmonton Formation of Alberta. The Ottawa Naturalist, **31**: 65–73. doi:10.4039/Ent50387a-11.

Lambe, L.M. 1920. The hadrosaur *Edmontosaurus* from the Upper Cretaceous of Alberta. Memoirs of the Canada Department of Mines, Geological Survey, **120**: 1–79.

Lang, A.H. 1947. Brule and Entrance map-areas, Alberta. Canadian Geological Survey Memoir 244. 1–65.

Langston, W. 1959. Alberta and fossil vertebrates. *In* Canadian Society of Petroleum Geologists, Ninth Annual Field Conference. Moose Mountain-Drumheller.

Lawton, T.F., and Bradford, B.A. 2011. Correlation and provenance of Upper Cretaceous (Campanian) fluvial strata, Utah, U.S.A., from Zircon U-Pb geochronology and petrography. Journal of Sedimentary Research, **81**: 495–512. doi:10.2110/jsr.2011.45.

Lockley, M.G., Nadon, G., and Currie, P.J. 2004. A diverse dinosaur-bird footprint assemblage from the Lance Formation, Upper Cretaceous, Eastern Wyoming: implications for ichnotaxonomy. Ichnos, **11**: 229–249. doi:10.1080/10420940490428625.

Mallon, J.C. 2019. Competition structured a Late Cretaceous megaherbivorous dinosaur assemblage. Scientific Reports, **9**: 1–19. doi:10.1038/s41598-019-51709-5. PMID: 30626917.

Mallon, J.C., Evans, D.C., Ryan, M.J., and Anderson, J.S. 2012. Megaherbivorous dinosaur turnover in the Dinosaur Park Formation (upper Campanian) of Alberta, Canada. Palaeogeography, Palaeoclimatology, Palaeoecology, **350–352**: 124–138. doi:10.1016/j.palaeo.2012.06.024. PMID: 23564975.

McCrea, R.T., Buckley, L.G., Plint, A.G., Currie, P.J., Haggart, J.W., Helm, C.W., and Pemberton, S.G. 2014. A review of vertebrate track-bearing formations from the Mesozoic and earliest Cenozoic of Western Canada with a description of a new theropod ichnospecies and reassignment of an avian ichnogenus. Fossil Footprints of Western North America. New Mexico Museum of Natural History & Science Bulletin, **62**: 5–94.

Mori, H., Drunkenmiller, P.S., and Erickson, G.M. 2016. A new Arctic hadrosaurid from the Prince Creek Formation (Lower Maastrichtian) of northern Alaska. Acta Palaeontologica Polonica, **61**: 15–32. doi:10.4202/app.00152.2015.

Pană, D.I., Elgr, R. and comp 2013. Geology of the Alberta Rocky Mountains and foothills; Energy Resources Conservation Board, ERCB/AGS Map 560, scale 1:500 000.

Pană, D.I., and van der Pluijm, B.A. 2014. Orogenic pulses in the Alberta Rocky Mountains: radiometric dating of major faults and comparison with the regional tectono-stratigraphic record. Bulletin of the Geological Society of America, **127**: 480–502. doi:10.1130/B31069.1.

Power, B.A., and Walker, R.G. 1996. Allostratigraphy of the Upper Cretaceous Lea Park–Belly River transition in central Alberta, Canada. Bulletin of Canadian Petroleum Geology, **44**: 14–38.

Prior, G.J., Hathway, B., Glombick, P.M., Pana, D.I., Banks, C.J., Hay, D.C., Schneider, C.L. Grobe, M. Elger, R. and Weiss, J.A. 2013. Bedrock Geology of Alberta, Alberta Energy Regulator, AER/AGS Map 600, scale 1:1 000 000.

Putnam, P.E. 1993. A multidisciplinary analysis of Belly River-Brazeau (Campanian) fluvial channel reservoirs in west-central Alberta, Canada. *In* Bulletin of Canadian Petroleum Geology.

Ramezani, J., Beveridge, T.L., Rogers, R.R., Eberth, D.A., and Roberts, E.M. 2022. Calibrating the zenith of dinosaur diversity in the Campanian of the Western Interior Basin by CA-ID-TIMS U–Pb geochronology. Scientific Reports, **12**: 1–20. doi:10.1038/s41598-022-19896-w.

Rogers, R.R., Eberth, D.A., and Ramezani, J. 2023. The "Judith River–Belly River problem" revisited (Montana-Alberta-Saskatchewan): new perspectives on the correlation of Campanian dinosaur-bearing strata based on a revised stratigraphic model updated with CA-ID-TIMS U-Pb geochronology. Geological Society of America Bulletin, **July**: 1–17. doi:10.1130/B36999.1.

Russell, D.A., and Chamney, T.P. 1967. Notes on the biostratigraphy of dinosaurian and microfossil faunas in the Edmonton Formation (Cretaceous), Alberta. National Museum of Canada, Natural History Papers, **35**: 1–22.

Sharpe, H.S. Powers, M.J. Dyer, A.D. Rhodes, M.M. McIntosh, A.P. Garros, A.P. Currie, P.J. and Funston, G.F. 2023. Craniomandibular anatomy of a juvenile specimen of Edmontosaurus regalis Lambe, 1917 clarifies issues in ontogeny and biogeography. Journal of Vertebrate Paleontology **43**: doi:10.1080/02724634.2024.2326644.

Simonetti, A., Heaman, L.M., Hartlaub, R.P., Creaser, R.A., MacHattie, T.G., and Böhm, C. 2005. U-Pb zircon dating by laser ablation-MC-ICP-MS using a new multiple ion counting Faraday collector array. Journal of Analytical Atomic Spectrometry, **20**: 677–686. doi:10.1039/b504465k.

Sláma, J., Košler, J., Condon, D.J., Crowley, J.L., Gerdes, A., Hanchar, J.M., et al. 2008. Plešovice zircon—a new natural reference material for U-Pb and Hf isotopic microanalysis. Chemical Geology, **249**: 1–35. doi:10.1016/j.chemgeo.2007.11.005.

Smith, M.E., Carroll, A.R., and Scott, J.J. 2015. Stratigraphy and river formation, of the Green Paleolimnology Western USA. *In* Stratigraphy and paleolimnology of the Green River Formation, western USA: syntheses in limnogeology. *Edited by* M.E. Smith and A.R. Carroll. Springer, Dordrecht, Netherlands. p. 355.

Smith, M.E., Carroll, A.R., and Singer, B.S. 2008. Synoptic reconstruction of a major ancient lake system: Eocene Green River Formation, western United States. Geological Society of America Bulletin, **120**: 54–84. doi:10.1130/B26073.1.

Söderlund, U., and Johansson, L. 2002. A simple way to extract baddeleyite (ZrO_2). Geochemistry, Geophysics, Geosystems, **3**(2). doi:10.1029/2001GC000212.

Sweet, A.R. 1987. Report on 55 samples from the Paskapoo, Coalspur and Brazeau formations from the Central Alberta Foothills (NTS 83C and F) as requested by T. Jerzykiewicz. Geological Survey of Canada, **ARS-1987-0**: 1–20.

Takasaki, R., Fiorillo, A.R., Tykoski, R.S., and Kobayashi, Y. 2020. Re-examination of the cranial osteology of the Arctic Alaskan hadrosaurine with implications for its taxonomic status. PLoS ONE, **15**: 1–31. doi:10.1371/journal.pone.0232410.

Vermeesch, P. 2018. IsoplotR: a free and open toolbox for geochronology. Geoscience Frontiers, **9**: 1479–1493. doi:10.1016/j.gsf.2018.04.001.

Voris, J.T., Zelenitsky, D.K., Therrien, F., and Tanaka, K. 2018. Dinosaur eggshells from the Lower Maastrichtian St. Mary River Formation of southern Alberta, Canada. Canadian Journal of Earth Sciences, **55**: 272–282. doi:10.1139/cjes-2017-0195.

Xing, H., Mallon, J.C., and Currie, M.L. 2017. Supplementary cranial description of the types of *Edmontosaurus regalis* (Ornithischia: Hadrosauridae), with comments on the phylogenetics and biogeography of Hadrosaurinae. PLoS ONE, **12**: 1–40. doi:10.1371/journal.pone.0175253.

Zubalich, R., Capozzi, R., Fanti, F., and Catuneanu, O. 2021. Evolution of the Western Interior Seaway in west-central Alberta (late Campanian, Canada): implications for hydrocarbon exploration. Marine and Petroleum Geology, **124**: 104779. doi:10.1016/j.marpetgeo.2020.104779.